

ON THE NATURE OF THE PROTOTYPE LBV AG CARINAE<sup>1</sup>  
I. FUNDAMENTAL PARAMETERS DURING VISUAL MINIMUM PHASES AND CHANGES IN THE  
BOLOMETRIC LUMINOSITY DURING THE S-DOR CYCLE

J. H. GROH<sup>2,3,4</sup>, D. J. HILLIER<sup>4</sup>, A. DAMINELI<sup>2</sup>, P. A. WHITELOCK<sup>5,6</sup>, F. MARANG<sup>5</sup>, AND C. ROSSI<sup>7</sup>

*ApJ*, in press

ABSTRACT

We present a detailed spectroscopic analysis of the luminous blue variable AG Carinae during the last two visual minimum phases of its S-Dor cycle (1985–1990 and 2000–2003). The analysis reveals an overabundance of He, N, and Na, and a depletion of H, C, and O, on the surface of AG Car, indicating the presence of CNO-processed material. Furthermore, the ratio N/O is higher on the stellar surface than in the nebula. We found that the minimum phases of AG Car are not equal to each other, since we derived a noticeable difference between the maximum effective temperature achieved during 1985–1990 (22,800 K) and 2000–2001 (17,000 K). Significant differences between the wind parameters in these two epochs were also noticed. While the wind terminal velocity was 300 km s<sup>-1</sup> in 1985–1990, it was as low as 105 km s<sup>-1</sup> in 2001. The mass-loss rate, however, was lower from 1985–1990 ( $1.5 \times 10^{-5} M_{\odot}\text{yr}^{-1}$ ) than from 2000–2001 ( $3.7 \times 10^{-5} M_{\odot}\text{yr}^{-1}$ ). We found that the wind of AG Car is significantly clumped ( $f \simeq 0.10 - 0.25$ ) and that clumps must be formed deep in the wind. We derived a bolometric luminosity of  $1.5 \times 10^6 L_{\odot}$  during both minimum phases which, contrary to the common assumption, decreases to  $1.0 \times 10^6 L_{\odot}$  as the star moves towards maximum flux in the V band. Assuming that the decrease in the bolometric luminosity of AG Car is due to the energy used to expand the outer layers of the star (Lamers 1995), we found that the expanding layers contain roughly  $0.6 - 2 M_{\odot}$ . Such an amount of mass is an order of magnitude lower than the nebular mass around AG Car, but is comparable to the nebular mass found around lower-luminosity LBVs and to that of the Little Homunculus of Eta Car. If such a large amount of mass is indeed involved in the S Dor-type variability, we speculate that such instability could be a failed Giant Eruption, with several solar masses never becoming unbound from the star.

*Subject headings:* stars: atmospheres — stars: mass loss — stars: variables: other — supergiants — stars: individual (AG Carinae) — stars: rotation

1. INTRODUCTION

Luminous Blue Variables (LBVs) are characterized as high-luminosity, blue (i.e. hot) massive stars showing photometric and spectroscopic variability (Conti 1984; Humphreys & Davidson 1994; van Genderen 2001; Clark et al. 2005). AG Carinae (=HD 94910,  $\alpha_{2000}=10:56:11.6$ ,  $\delta_{2000}=-60:27:12.8$ ), one of the brightest, most famous, and most variable LBVs, is considered one of the proto-

types of this class, presenting all of the above characteristics.

Intense observing campaigns in the past decades have determined many of the characteristics of AG Car. The star has photometric, spectroscopic, and polarimetric variability on a range of timescales spanning days to decades. The optical photometric variability of AG Car was analyzed in detail by van Genderen et al. (1988), van Genderen et al. (1990), Sterken et al. (1996), and van Genderen et al. (1997a). These authors determined that AG Car has strong photometric changes of up to 2.5 mag in the V band on a timescale of about 5–10 years, which are attributed to the S Dor-type variability (van Genderen 1982; van Genderen et al. 1997b; van Genderen 2001), and *should not* be confused with giant eruptions similar to that experienced by Eta Carinae in the 1840's. Superimposed on these variations, 0.1 – 0.5 mag changes are present on a timescale of 371 days (van Genderen et al. 1997a), and photometric microvariability (0.01 – 0.02 mag) with a timescale of 10–14 days has been recorded during visual minimum (van Genderen et al. 1988, 1990). Whitelock et al. (1983) reported the near-infrared *JHKL* lightcurve of AG Car between 1974–1982, showing that the amplitude of the light variations in the near-infrared is comparable to what is seen in the V band.

AG Car is also a spectroscopic variable (Caputo & Viotti 1970; Humphreys 1970; Viotti 1971; Wolf & Stahl

Electronic address: jgroh@mpifr-bonn.mpg.de

<sup>1</sup> Based on observations made with the 1.6m telescope at the Observatório Pico dos Dias (OPD/LNA, Brazil), with the 1.52m telescope and 8m Very Large Telescope at the European Southern Observatory (ESO, Chile), with the International Ultraviolet Explorer (IUE) satellite, at the South African Astronomical Observatory (SAAO), and with the NASA–CNES–CSA Far Ultraviolet Spectroscopic Explorer (FUSE), which is operated for NASA by the Johns Hopkins University under NASA contract NAS5–32985.

<sup>2</sup> Instituto de Astronomia, Geofísica e Ciências Atmosféricas, Universidade de São Paulo, Rua do Matão 1226, Cidade Universitária, 05508-900, São Paulo, SP, Brazil

<sup>3</sup> Max-Planck-Institut für Radioastronomie, Auf dem Hügel 69, D-53121 Bonn, Germany (present address)

<sup>4</sup> Department of Physics and Astronomy, University of Pittsburgh, 3941 O'Hara Street, Pittsburgh, PA, 15260, USA

<sup>5</sup> South African Astronomical Observatory, PO Box 9, 7935 Observatory, South Africa

<sup>6</sup> National Astrophysics and Space Science Programme, Department of Mathematics and Applied Mathematics and Department of Astronomy, University of Cape Town, 7701 Rondebosch, South Africa

<sup>7</sup> Università di Roma "La Sapienza", Piazzale A. Moro 5, 00185 Roma, Italy

1982), and the variability on timescale of years has been analyzed in different spectral regions: ultraviolet (Leitherer et al. 1994; Shore et al. 1996), optical (Leitherer et al. 1994; Stahl et al. 2001), and near-infrared (Groh et al. 2007). During the epochs of minimum in the visual lightcurve (hereafter referred to as “minimum”;  $m_V \simeq 8.1$ ; van Genderen 2001), the star is relatively hot and has a WN11 spectral type (Smith et al. 1994), showing strong He I, H I, and N II lines in emission, weak He II 4686 Å emission, and Si IV 4088–4116 Å absorption (Stahl 1986; Smith et al. 1994; Walborn & Fitzpatrick 2000; Groh et al. 2006). During the maximum epochs of the lightcurve ( $m_V \sim 6.0$ ; van Genderen 2001) the star is cooler, and the spectrum is reminiscent of that of extreme A-type hypergiants, with strong emission of H I, Fe II, and Ti II lines (Wolf & Stahl 1982; Stahl et al. 2001). The transition between both phases is characterized by the appearance of peculiar features in the spectrum, such as absorption-line splitting, strong electron-scattering wings in He I and Fe II lines, and apparent inverse P-Cygni profiles in He I lines (Leitherer et al. 1994; Stahl et al. 2001). The variable and high polarization degree measured in AG Car motivated spectropolarimetric monitoring (Schulte-Ladbeck et al. 1994; Leitherer et al. 1994; Schulte-Ladbeck et al. 1997; Davies et al. 2005, 2006, 2008).

The presence of a massive, bipolar circumstellar nebula around AG Car is a testament that a recent ( $t < 10^4$  years) phase of high mass loss has occurred. The morphology and kinematics of the nebula were analyzed by Nota et al. (1992) and Nota et al. (1995), who determined a dynamical age of  $8.5 \times 10^3$  years and a high mass of ionized nebular material ( $\sim 4.2 M_\odot$ ), which is likely composed of ejecta from the central star (Lamers et al. 2001). The nebular abundances were obtained by Mitra & Dufour (1990), de Freitas Pacheco et al. (1992), and Smith et al. (1997), showing evidence of moderate nitrogen enrichment. Properties of the circumstellar nebula were also studied in the mid- and far-infrared, revealing an incredibly high dust mass of  $\sim 0.25 M_\odot$  (Voors et al. 2000), dust temperature between 76–99 K (Voors et al. 2000), and the presence of large grains of  $\sim 1 \mu\text{m}$  in order to explain the far-IR excess (Voors et al. 2000; Hyland & Robinson 1991). Assuming a normal gas-to-dust ratio of 100, the total nebular mass of AG Car could be as high as  $\sim 30 M_\odot$  (Voors et al. 2000), which would be of the order of, *or even higher than*, the mass of the Homunculus nebula around Eta Car obtained by Smith et al. (2003). At the time when the AG Car nebula was ejected, the interstellar bubble around the central star likely contained a negligible amount of material compared to the total mass of the nebula (Lamers et al. 2001), implying that most of the nebular mass was ejected by the central star.

While insights into the nature of AG Car have been obtained through the quantitative works of Leitherer et al. (1994) and Stahl et al. (2001), the stellar and wind parameters of AG Car at each epoch along the S Dor-type variability cycle (hereafter S Dor cycle) are not completely constrained. Furthermore, it is currently feasible to include important physical processes in the radiative transfer codes which have had a key impact on the determination of stellar parameters of O-type (e.g. Crowther et al. 2002; Hillier et al. 2003; Bouret et al. 2003, 2005;

Martins et al. 2005; Puls et al. 2006) and Wolf-Rayet stars (e.g. Hillier & Miller 1999; Hamann et al. 2006; Crowther 2007; Gräfener & Hamann 2008). The inclusion of full line blanketing due to 100 000s of lines, wind clumping and charge-exchange reaction, and the simultaneous treatment of the wind and photosphere in the model will considerably affect the emerging model spectrum. Together with the possibility of doing a full synthesis of the spectrum and thus using more diagnostic lines, our analysis should provide a more accurate determination of the stellar and wind properties of AG Car.

This work is the first in a series of papers resulting from a long-term multi-wavelength spectroscopic and photometric monitoring campaign to follow AG Car during the last two decades. In a previous paper (Groh et al. 2006), we presented quantitative evidence that AG Car had a high rotational velocity during the minimum phase of 2000–2003 and, for the first time, we showed that LBVs can be fast rotators. In this work, we present, interpret, and discuss the results obtained from observations in the last two well-documented minimum phases of AG Car; namely, during the years of 1985–1990 and 2000–2003. Although it is subjective to define the beginning and end of minimum phases for stars which have irregular variations, such as AG Car, we analyze in this paper epochs when the star was fainter than  $V = 7$ . This criterion corresponds roughly to epochs when He I lines were relatively strong and displayed a classical P-Cygni profile, and time-dependent effects were minimized.

This paper is organized as follows. In Sect. 2 we present the photometric and spectroscopic observations obtained during the last two minimum phases of AG Car, while in Sect. 3 we describe the spectroscopic evolution during those minima. In Sect. 4 we introduce the main characteristics of CMFGEN (Hillier & Miller 1998), the radiative transfer code used to derive the fundamental parameters of AG Car. Sect. 5 briefly discusses the distance of AG Car, and how the parameters are affected by that quantity. The surface chemical abundances, mass-loss rate, wind terminal velocity, stellar temperature, stellar radius, and stellar luminosity for each minimum are presented in Sect. 6, and the interpretation and discussion can be found in Sect. 7. The conclusions of this paper, which suggest key changes in the current paradigm for interpreting the LBV phase and their S-Dor cycles, in particular the minimum phases, are summarized in Sect. 8.

The present work will be followed by two accompanying papers. In Paper II we will discuss the evolutionary status, current mass, proximity to the Eddington limit, and whether the bi-stability mechanism is present in AG Car. The evolution of the fundamental parameters of AG Car during the full S Dor cycle will be analyzed, in detail, in Paper III.

## 2. OBSERVATIONS

### 2.1. Photometry

The optical photometry of AG Car was obtained from published data from the Long-term Photometry of Variables project (LTPV; Sterken 1983; Manfroid et al. 1991; Sterken et al. 1993; Spoon et al. 1994; Manfroid et al. 1995; Sterken et al. 1995), accessed through the online

catalog of VizieR/CDS<sup>8</sup>. The observations were acquired using *uvby* Strömrgren filters on the ESO 50 cm La Silla telescope, and the typical individual errors are between 0.003–0.006 mag. The reader is referred to the aforementioned papers for further details about the observational setup, data reduction, and calibration. Since the LTPV project was not active after 1994, CCD *V* magnitudes from 2000–2003 were obtained from the ASAS-3 project (Pojmanski 2002). The ASAS-3 data were averaged in bins of 15 days, and only high quality (grade A) data were used. Although the ASAS-3 magnitudes were measured using large apertures (75"), AG Car is by far the dominant source of light in the field.

For comparative purposes, estimates of the visual magnitude of AG Car from 1981–2004 were compiled from the AAVSO archive (A. A. Heiden 2007, private communication). When both AAVSO and ASAS-3 data were available at a given epoch, their 15-day averaged magnitudes were compatible within  $\sim 0.1$  mag. However, the 15-day averaged AAVSO visual lightcurve does not exactly match the more precise photoelectric *V*-band lightcurve presented by van Genderen (2001), in particular during maximum. This is not surprising, since the AAVSO sample is composed by visual estimates (i.e. by eye) from different observers, and the uncertainty could be large during maximum. We estimate that the 15-day averaged AAVSO magnitudes have an uncertainty of 0.1–0.2 mag during minimum, and perhaps even more during maximum. Note that the AAVSO magnitudes are presented in this paper only for the purpose of illustrating the general behavior of AG Car during 1981–2004, and due to their relatively low accuracy they were not used to derive a *V*-band flux.

The near-infrared photometry was obtained using the 75cm reflector telescope from the South African Astronomical Observatory (SAAO) and *JHKL* filters. The SAAO photometric system is described by Carter (1990), and the instrument used was an *MkII* photometer with a 36" aperture. The typical error for each individual measurement is 0.02 mag in the *J*, *H*, and *K* bands, and 0.05 mag in the *L* band. In principle, the large aperture used could include some contribution from the bipolar nebula around AG Car. However, magnitudes obtained with diaphragm apertures of 54", 36", 24", and 12" do not present significant differences, indicating that the nebular contribution is negligible (Whitelock et al. 1983).

Figure 1 displays the AG Car lightcurve encompassing its last two minimum phases measured in the *K*-band, the photoelectric Strömrgren *y*-band photometry obtained by the LTPV project, the ASAS-3 *V*-band observations, and the photoelectric lightcurve presented by van Genderen (2001). For comparison, 15-day averaged visual estimates made by the AAVSO observers are also shown. Table 1 summarizes the photometry of AG Car used in this paper. The epochs from the first column correspond to those when spectroscopic data, during minimum, were available. The magnitudes were obtained through linear interpolation between the closest dates which had available photometry.

Fortunately, the time samplings of both the near-IR lightcurve and the optical photometry are suitable to follow the variability of AG Car on timescales of the order

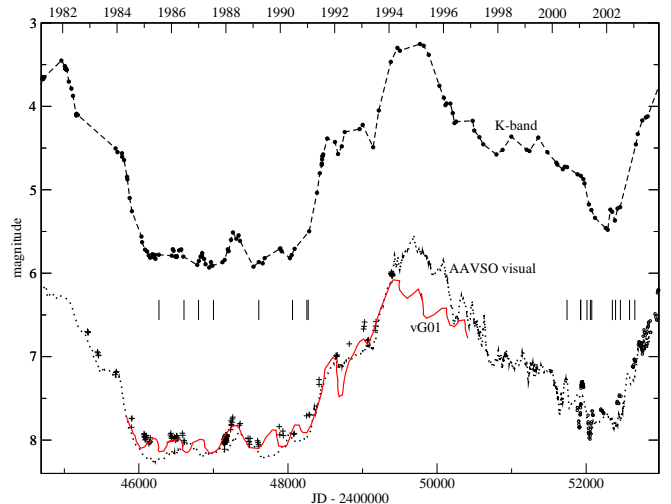


FIG. 1.— AG Car photoelectric lightcurve from 1982 to 2004 obtained in the *K*-band (filled circles connected by a dashed line), in the Strömrgren *y*-band by the LTPV project (crosses; Sterken 1983; Manfroid et al. 1991; Sterken et al. 1993; Spoon et al. 1994; Manfroid et al. 1995; Sterken et al. 1995), and in the *V*-band by the ASAS-3 project (open circles; Pojmanski 2002). For illustrative purposes, the schematic *V*-band photoelectric lightcurve presented by van Genderen (2001) (red solid line) and the 15-day averaged visual magnitudes measured by the AAVSO observers (dotted line; A. A. Heiden 2007, private communication) are also shown. The vertical lines mark epochs when spectroscopic data, during minimum, were available (see Table 2).

of months, and match the dates when the spectra were taken relatively well (Table 1). Variability on timescales shorter than a couple of months is definitely present in AG Car (van Genderen 2001), however with an amplitude of  $\lesssim 0.2$  mag (van Genderen et al. 1988), and thus do not affect the results obtained in this paper.

## 2.2. Spectroscopy

### 2.2.1. Minimum of 1985–1990

Flux-calibrated ultraviolet spectra of AG Car were obtained by the *International Ultraviolet Explorer* (IUE) satellite in the region 1150–3120 Å and gathered through the *Space Telescope Science Institute* (STSCI) public-data archive. The IUE absolute-flux calibration is precise to about 5% (degrading in the edges of the spectral range), which is adequate for our purposes. AG Car was observed in various epochs during the 1985–1990 minimum with the SWP and LWP high-resolution cameras, with  $R \simeq 15,000$  in the wavelength range of 1150–3200 Å (Table 2, see also Leitherer et al. 1994; Shore et al. 1996).

Optical spectra of AG Car were obtained using different telescopes in the southern hemisphere. The Echelle spectrograph mounted on the 1.4m CAT/ESO (Chile) telescope was used to collect high-resolution spectra from 1986 June to 1991 January around  $H\alpha$ , He I 5876 Å, and He II 4686 Å, with  $R=60,000$ . Most of these data have been described elsewhere (Bandiera et al. 1989; Viotti et al. 1991; Leitherer et al. 1994). Lower resolution data between 3800–4900 Å were obtained using the 1m CTIO/Yale telescope and were discussed by Walborn & Fitzpatrick (2000). Additional lower-resolution observations using the longslit Cassegrain spectrograph on the 1.52m ESO/La Silla telescope were made on 1990 June

<sup>8</sup> <http://vizier.u-strasbg.fr/viz-bin/VizieR>

TABLE 1  
PHOTOMETRY OF AG CAR INTERPOLATED TO EPOCHS WHEN SPECTRA WERE AVAILABLE DURING MINIMUM<sup>a</sup>

Epoch	<i>u</i> (0.01)	<i>v</i> (0.01)	<i>b</i> (0.01)	<i>y</i> (0.01)	visual (0.1)	<i>V</i> (0.05)	<i>J</i> (0.02)	<i>H</i> (0.02)	<i>K</i> (0.02)	<i>L</i> (0.05)	$\Delta$ LTPV <sup>b</sup> (days)	$\Delta$ V <sup>b</sup> (days)	$\Delta$ NIR <sup>b</sup> (days)
1985 Jul 19	8.94	8.72	8.37	7.96	8.2	...	6.45	6.13	5.78	5.34	112	...	-3
1986 Jun 17	9.04	8.78	8.41	7.98	8.1	...	6.47	6.12	5.80	5.35	-7	...	1
1986 Jun 18	9.05	8.79	8.41	7.98	8.1	...	6.47	6.12	5.80	5.35	-6	...	2
1986 Jun 23	9.07	8.81	8.43	8.00	8.1	...	6.47	6.13	5.81	5.36	-1	...	7
1987 Jan 05	9.03	8.81	8.43	8.03	8.1	...	6.52	6.19	5.86	5.36	192	...	-4
1987 Jun 10	9.00	8.81	8.43	8.03	8.2	...	6.57	6.24	5.93	5.63	-183	...	12
1987 Jul 24	8.99	8.80	8.43	8.03	8.1	...	6.57	6.23	5.91	5.50	-139	...	14
1989 Mar 26	8.98	8.83	8.45	8.07	8.2	...	6.54	6.19	5.87	5.22	1	...	2
1989 Dec 23	8.79	8.63	8.26	7.85	8.1	...	6.38	6.05	5.71	5.25	1	...	-8
1990 Apr 30	8.84	8.72	8.36	7.94	7.9	...	6.42	6.11	5.81	5.37	-64	...	-15
1990 Jun 16	8.88	8.72	8.35	7.93	8.0	...	6.41	6.08	5.77	5.32	-17	...	8
1990 Jun 18	8.88	8.72	8.35	7.93	8.0	...	6.41	6.07	5.76	5.32	-15	...	10
1990 Aug 07	8.83	8.67	8.29	7.89	8.0	...	6.32	5.99	5.69	5.24	26	...	20
1990 Dec 22	8.66	8.51	8.14	7.71	8.0	...	6.18	5.86	5.54	5.12	-1	...	-37
1990 Dec 28	8.66	8.50	8.13	7.71	8.0	...	6.17	5.85	5.53	5.12	4	...	-31
1991 Jan 21	8.65	8.48	8.12	7.69	7.9	...	6.15	5.83	5.51	5.10	-4	...	-7
2000 Jul 18	...	...	...	...	7.3	...	5.54	5.15	4.73	4.18	...	...	0
2000 Dec 12	...	...	...	...	7.5	7.67	5.58	5.20	4.82	4.29	...	2	5
2001 Jan 17	...	...	...	...	7.5	7.57	5.57	5.21	4.83	4.32	...	0	-3
2001 Apr 12	...	...	...	...	7.7	7.63	5.80	5.45	5.07	4.55	...	-13	-26
2001 May 27	...	...	...	...	7.9	7.90	5.91	5.58	5.21	4.71	...	0	-14
2001 Jun 10	...	...	...	...	7.9	7.78	5.94	5.61	5.24	4.75	...	0	0
2001 Jun 15	...	...	...	...	7.9	7.71	5.95	5.62	5.25	4.76	...	-4	4
2002 Mar 17	...	...	...	...	7.7	7.60	5.93	5.60	5.27	4.93	...	-60	1
2002 Apr 30	...	...	...	...	7.8	7.57	6.01	5.68	5.34	4.92	...	-16	7
2002 Jul 04	...	...	...	...	7.8	7.47	5.88	5.54	5.20	4.79	...	-8	2
2002 Jul 20	...	...	...	...	7.7	7.46	5.84	5.49	5.14	4.73	...	7	18
2002 Nov 04	...	...	...	...	7.2	7.20	5.51	5.12	4.76	4.30	...	-39	-85
2003 Jan 11	...	...	...	...	7.2	7.03	5.31	4.89	4.52	4.03	...	0	-17

<sup>a</sup> Photometric errors are indicated in parenthesis. References: *uvby* Strömgen=LTPV project (Sterken 1983; Manfroid et al. 1991; Sterken et al. 1993; Spoon et al. 1994; Manfroid et al. 1995; Sterken et al. 1995); AAVSO visual=A. A. Heiden 2007, private communication; ASAS V-band=Pojmanski (2002); JHKL=SAAO (Whitelock et al. 1983; this work).

<sup>b</sup> Time delay between the epochs when spectroscopic and photometric observations were obtained ( $JD_{\text{spec}} - JD_{\text{phot}}$ ).

18–19 between 4330–4870 Å ( $R=2300$ ) and 6200–7270 Å ( $R=1700$ ), and were described by Viotti et al. (1993).

It was not possible to obtain a precise continuum normalization of the Echelle data around H $\alpha$  since the spectral coverage was very small and the electron scattering wings were very extended. Therefore, we scaled the Echelle spectra in flux in order to match the electron-scattering wings of the longslit data, as described by Leitherer et al. (1994). We conservatively estimate that the uncertainty in the continuum after this procedure is at most  $\sim 5\%$ . The same procedure could not be applied to the Echelle spectra around He I 5876 Å and, as a consequence, the strength of the electron scattering wings are not reliable, and are likely underestimated, around this line.

Additionally, the near-infrared region around 9950–10200 Å was covered by CCD observations made on the 1.6m telescope of the Observatório Pico dos Dias (OPD/LNA, Brazil) using the Coude spectrograph. The spectra typically have  $R \simeq 10,000$ , and the data reduction was accomplished using standard IRAF tasks for bias subtraction, flat-field correction, extraction of the spectrum, wavelength calibration, and continuum normalization. Those spectra were also published by Leitherer et al. (1994), where further details can be found.

### 2.2.2. Minimum of 2000–2003

During this minimum we used the Fiber-fed Extended Range Optical Spectrograph (FEROS; Kaufer et al. 1999) mounted on the 1.52 m telescope of ESO/La Silla

(Chile) to obtain spectra between 2001 January and 2002 March. The instrumental configuration provided spectral coverage between 3600–9200 Å at  $R=48,000$ , and the data was reduced using the FEROS pipeline (Stahl et al. 1999). We also used data obtained on 2003 January 11 with the UV-visual Echelle Spectrograph (UVES) mounted on the ESO 8m Very Large Telescope (VLT, program 266.D-5655, Bagnulo et al. 2003). The resolution provided by UVES was  $R = 80,000$  in the wavelength range 3000–10400 Å.

We used the near-infrared camera CamIV on the 1.6m telescope of OPD/LNA (Brazil) to obtain long-slit spectra of AG Car in the wavelength range 10450–11000 Å ( $R = 7000$ ) in 2001 June, 2002 July, and 2002 November. Further details on the observational setup and data reduction are given in Groh et al. (2007), where the data are also discussed.

With the decommissioning of IUE, no ultraviolet monitoring of the star was possible during the 2000–2003 minimum. Fortunately, a *Far Ultraviolet Spectroscopic Explorer* (FUSE) visit occurred in 2001 May 27, covering the far-ultraviolet region between 900–1180 Å ( $R = 20,000$ ). The FUSE spectrum was obtained from the online FUSE public-data archive.

The spectroscopic observations obtained during minimum are summarized in Table 2.

## 3. SPECTROSCOPIC VARIABILITY OF AG CAR DURING MINIMUM

TABLE 2  
JOURNAL OF SPECTROSCOPIC OBSERVATIONS OF AG CAR DURING  
MINIMUM

Date	Telescope	Spectral Range ( $\text{\AA}$ )	$R$
1985 July 19	IUE SWP	1180–1900	18,000
1986 June 17	1.4m ESO	5860–5910	60,000
1986 June 18	1.4m ESO	6532–6588	60,000
1986 June 23	IUE SWP	1180–1900	18,000
1986 June 23	IUE LWP	1800–3150	13,000
1987 January 05	1.4m ESO	5860–5910	60,000
1987 January 05	1.4m ESO	6532–6588	60,000
1987 June 10	1.4m ESO	3917–3947	60,000
1987 June 10	1.4m ESO	6532–6588	60,000
1987 July 24	IUE SWP	1180–1900	18,000
1987 July 24	IUE LWP	1800–3150	13,000
1989 March 26	1m CTIO/Yale	3800–4900	3000
1989 December 23	IUE SWP	1180–1900	18,000
1989 December 23	IUE LWP	1800–3150	13,000
1990 April 30	IUE SWP	1180–1900	400
1990 June 16	1.6m LNA	9950–10200	10,000
1990 June 18	1.52m ESO	4330–4870	2300
1990 June 18	1.52m ESO	6200–7270	1700
1990 August 07	IUE LWP	1800–3150	270
1990 December 22	1.6m LNA	9970–10080	10,000
1990 December 28	1.6m LNA	6490–6710	10,000
1991 January 21	1.4m ESO	4550–4750	60,000
2000 July 18	1.6m LNA	9950–10200	10,000
2000 July 18	1.6m LNA	6350–7100	10,000
2000 December 12	1.6m LNA	6350–7100	10,000
2001 January 17	1.52m ESO	3600–9200	48,000
2001 April 12	1.52m ESO	3600–9200	48,000
2001 May 27	FUSE	900–1180	20000
2001 June 10	1.6m LNA	10450–11000	7000
2001 June 15	1.52m ESO	3600–9200	48,000
2002 March 17	1.52m ESO	3600–9200	48,000
2002 April 30	1.6m LNA	10450–11000	7000
2002 July 04	1.52m ESO	3600–9200	48,000
2002 July 20	1.6m LNA	10450–11000	7000
2002 November 04	1.6m LNA	10450–11100	7000
2003 January 11	8m ESO/VLT	3000–10400	80,000

In this Section we present the spectroscopic evolution of AG Car during minimum epochs. Since other WN9–WN11 stars also display variability in the spectrum on timescales of years (McGregor et al. 1988b; Crowther 1997; Groh et al. 2007), investigating the variability behavior of AG Car might provide insights on the evolutionary link between LBVs and WN9–WN11 stars and on the physical mechanism which drives the S-Dor variability.

### 3.1. Minimum of 1985–1990

Leitherer et al. (1994) monitored the ultraviolet spectrum during the minimum of 1985–1990 and concluded that little or no variability was present. Indeed, the low level of variability is consistent with the visual lightcurve (Fig. 1), which shows only low-amplitude photometric variability of  $\sim 0.1 - 0.3$  mag during 1985–1990 (van Genderen et al. 1988, 1990; Leitherer et al. 1994; Stahl et al. 2001). The evolution of the optical spectrum from the end of the minimum (1990 December) until epochs on the rise to the lightcurve maximum (1992 June) was also followed by Leitherer et al. (1994).

Here we draw our attention to the evolution of the optical spectrum and photometry inside the 1985–1990 minimum. Spectra around He II 4686  $\text{\AA}$  were available only during 1989–1991 and are shown in Fig. 2. These data clearly show that He II 4686  $\text{\AA}$  became progressively

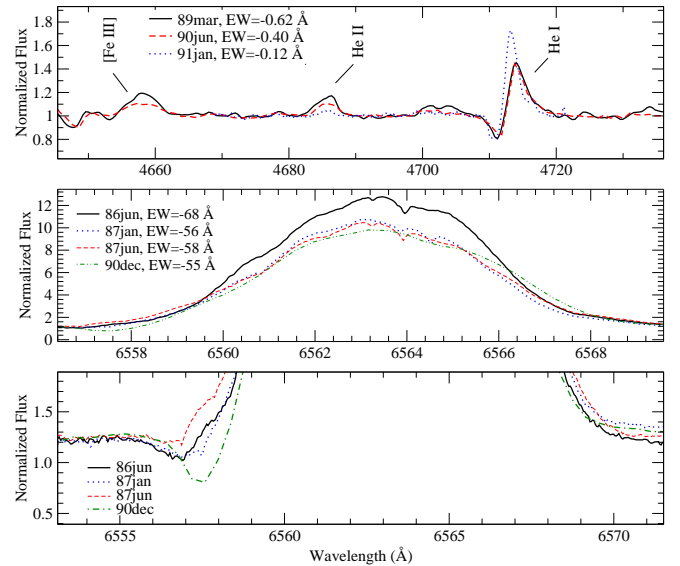


FIG. 2.— *Top*: AG Car spectrum around [Fe III] 4657  $\text{\AA}$  and He II 4686  $\text{\AA}$ , obtained in 1989 March (black solid line), 1990 June (red dashed), and 1991 January (blue dotted). The resolution of the spectra obtained in 1989 March and 1991 January were adjusted to the same resolution as the spectrum from 1990 June ( $R = 2300$ ). Quoted EWs refer to He II 4686  $\text{\AA}$ , and have an error of  $\sim 0.03$   $\text{\AA}$ . *Middle*: AG Car spectrum around  $H\alpha$  obtained in 1986 June (black solid line), 1987 January (blue dotted), 1987 June (red dashed), and 1990 December (green dot-dashed). Quoted EWs refer to the emission component of  $H\alpha$ , and have an error of  $\sim 2$   $\text{\AA}$  which is dominated by the uncertainty in the continuum level. *Bottom*: Zoom in around the variable P-Cygni absorption component that appears during some epochs, indicating changes in the ionization structure of hydrogen in the outer wind, as suggested by Crowther (1997) to explain a similar behavior seen in the LBV candidate He3-519. The offset of the continuum level from 1.0 is due to the strong  $H\alpha$  electron scattering wings.

weaker from 1989 until 1991, indicating a decrease of the effective temperature. The high-ionization line of [Fe III] 4657  $\text{\AA}$  also became slightly weaker from 1989 March until 1990 June.

The  $H\alpha$  line was followed with a better time sampling than He II 4686  $\text{\AA}$  (Fig. 2). It can be noticed that moderate variations were present in the emission component of  $H\alpha$ , with a decrease in the equivalent width (EW) from 1986 June to 1987 January. The EW of  $H\alpha$  varied from  $-68 \pm 2$   $\text{\AA}$  in 1986 June to  $-56 \pm 2$   $\text{\AA}$  in 1987 January (Fig. 2), and then remained approximately constant until 1990 December. On the other hand, the  $y$ -band magnitude was 8.00 mag in 1986 June, remained roughly constant during 1987, and only changed significantly to 7.71 mag in 1990 December (Fig. 1). Therefore, the changes in the emission component in  $H\alpha$  can be explained by a net increase in the continuum emission compared to the line emission only in 1990 December – on the other hand, the line emission was indeed stronger in 1986 June compared to the rest of the minimum.

In addition to the changes in the emission component, a weak P-Cygni absorption in  $H\alpha$  developed during some epochs between 1985–1990. Interestingly, a similar behavior was previously noticed in the LBV candidate He 3-519 (Crowther 1997), whose spectrum is remarkably similar to AG Car’s during the 1985–1990 minimum (Smith et al. 1994; Walborn & Fitzpatrick 2000). Crowther (1997) suggested that this behavior is due to changes

in the ionization structure of hydrogen in the outer parts of the wind. In this scenario, the absorption component seen in H $\alpha$  appears when a fraction of hydrogen recombines in the outer part of the wind and disappears when hydrogen is mainly ionized. A similar behavior has also been detected in the LBV P Cygni (Pauldrach & Puls 1990; Najarro et al. 1997).

Comparing the evolution of the emission and absorption components of H $\alpha$ , we suggest that the stellar and/or wind parameters are variable even during minimum epochs, and radiative transfer models are needed to quantify these changes. The detailed analysis of the 1985–1990 minimum spectra will be presented in Sect. 6.2.

### 3.2. Minimum of 2000–2003

Figure 3 displays the evolution of the optical spectrum of AG Car between 3690–8850 Å. The variability in the near-infrared region from 10500–11000 Å was presented by Groh et al. (2007).

In general, the spectral lines became broader from 2001 April to 2002 March and then narrower in 2003 January, indicating changes in the wind terminal velocity as a function of temperature. That behavior is interpreted as due to the fast rotation of AG Car (Groh et al. 2006), but might also be caused by the time-dependent nature of the velocity field. The hydrogen Balmer and Paschen lines (Fig. 3) show a significant change in strength and line profile inside the minimum: they became weaker from 2001 April to 2002 March and then stronger in 2003 January, indicating changes in the wind density. He II 4686 Å is very weak during the minimum of 2000–2003, with  $EW \simeq -100 \pm 10$  mÅ in 2001 April and 2001 June spectra, and  $EW \simeq -80 \pm 30$  mÅ in the 2002 March spectrum. He II 4686 Å is absent in the 2003 UVES spectrum, with an upper limit of 15 mÅ. Comparatively, this line is readily identified in the spectrum of AG Car during the 1985–1990 minimum (Fig. 2; Stahl 1986; Viotti et al. 1993; Leitherer et al. 1994; Smith et al. 1994; Walborn & Fitzpatrick 2000; Stahl et al. 2001).

Meanwhile, the He I, Fe III, and N II lines became weaker from 2001 to 2003, while the very weak Fe II and Mg II lines seen in the 2001 and 2002 spectra are prominent in the data from 2003. This behavior indicates that the effective temperature was decreasing from 2001 to 2003. Therefore, the above picture is consistent with the star moving out of minimum from 2001 to 2003, as suggested by the visual lightcurve (Fig. 1).

Interestingly, multiple absorption components appeared during 2001–2003 in the hydrogen, Fe II, and Ni II lines (Fig. 4), and are reminiscent of what was seen during 1991–1993 (Leitherer et al. 1994; Stahl et al. 2001) when the star was also moving towards maximum. Three absorption components in the Fe II lines can be securely identified in the data from 2000–2003, and they are centered at  $-72$ ,  $-101$ , and  $-148$  km s $^{-1}$  in the FEROS spectra from 2001–2002. These absorption components change in velocity and in strength in timescales as short as 1 year, as first noted by Stahl et al. (2001). Our data also present a similar behavior, and in the 2003 UVES spectrum, these absorption components shift to  $-74$ ,  $-112$ , and  $-153$  km s $^{-1}$ . An additional absorption component centered at  $-202$  km s $^{-1}$  is also present in

the Fe II and hydrogen Balmer lines in 2003.

The  $-72$  km s $^{-1}$  component could arguably be formed in the distant circumstellar nebula, which has an expansion velocity of  $\sim 70$  km s $^{-1}$  (Nota et al. 1992), but that component is not observed at all epochs (Leitherer et al. 1994; Stahl et al. 2001, this work). The other multiple absorption components are unlikely to be formed in the distant circumstellar nebula of AG Car, since they change in velocity and are approximately centered at the wind terminal velocity found in previous epochs. Thus, the multiple absorption components in AG Car are likely not reminiscent of the multiple ejecta absorption components seen in the massive LBV Eta Carinae (Gull et al. 2005; Nielsen et al. 2005; Johansson et al. 2005; Gull et al. 2006). We support the scenario, proposed by Stahl et al. (2001), that the multiple-absorption features are formed much closer to the star and are due to regions in the wind which have a density decrease (or enhancement) due to the temporal variability of the star. Indeed, this behavior is predicted by detailed radiative transfer models which include time-dependent effects (Groh et al. 2008; J. H. Groh et al. 2009, in preparation).

## 4. THE MODEL

To analyze the spectra of AG Car, we used the radiative transfer code CMFGEN (Hillier 1987, 1990; Hillier & Miller 1998, 1999; Busche & Hillier 2005), which has been successfully used to model the spectrum of LBVs and related objects (Smith et al. 1994; Najarro et al. 1994, 1997, 2009; Najarro 2001; Hillier et al. 1998, 2001, 2006; Figer et al. 1998; Drissen et al. 2001; Bresolin et al. 2002; Marcolino et al. 2007). The code has been extensively discussed in the aforementioned references, and below we concisely describe the main characteristics of the code.

CMFGEN assumes an spherical-symmetric, steady-state outflow, and computes continuum and line formation in the non-LTE regime. Each model is defined by the hydrostatic stellar radius  $R_*$ , the luminosity  $L_*$ , the mass-loss rate  $\dot{M}$ , the wind terminal velocity  $v_\infty$ , the stellar mass  $M$ , and by the abundances  $Z_i$  of the included species. We define the hydrostatic radius  $R_*$  as the radius where the velocity is  $v(R_*) = v_{\text{sonic}}/3$ , in order to avoid any effects due to the strong wind in determination of  $R_*$ , which is the case for  $v \gtrsim v_{\text{sonic}}/3$ . Thus, the velocity of the hydrostatic core, where  $R_*$  and  $T_*$  are defined, is typically  $4 - 5$  km s $^{-1}$  for AG Car during minimum.

CMFGEN does not solve the hydrodynamic equations of the wind, and therefore, a velocity law  $v(r)$  has to be assumed a priori. In CMFGEN, the velocity law is parameterized either by a single beta-type law or by a two-beta velocity law which is modified at depth to reach a hydrostatic structure. The stellar mass  $M$  is needed to compute the density structure below and close to the sonic point, and therefore changes in  $M$  might affect the spectroscopic analysis. In this paper we assume  $M = 70 M_\odot$ , since lower values of  $M$  would imply that the star is above the Eddington limit modified by rotation (Paper II). A thorough discussion on the impact of  $M$  on the spectral analysis will be provided in Paper II. The velocity structure below the sonic point is iterated to fulfill the wind momentum equation within 10% for  $v \lesssim 8$  km s $^{-1}$ . A beta-type law is joined to this structure just below the sonic point. Although the code solves for

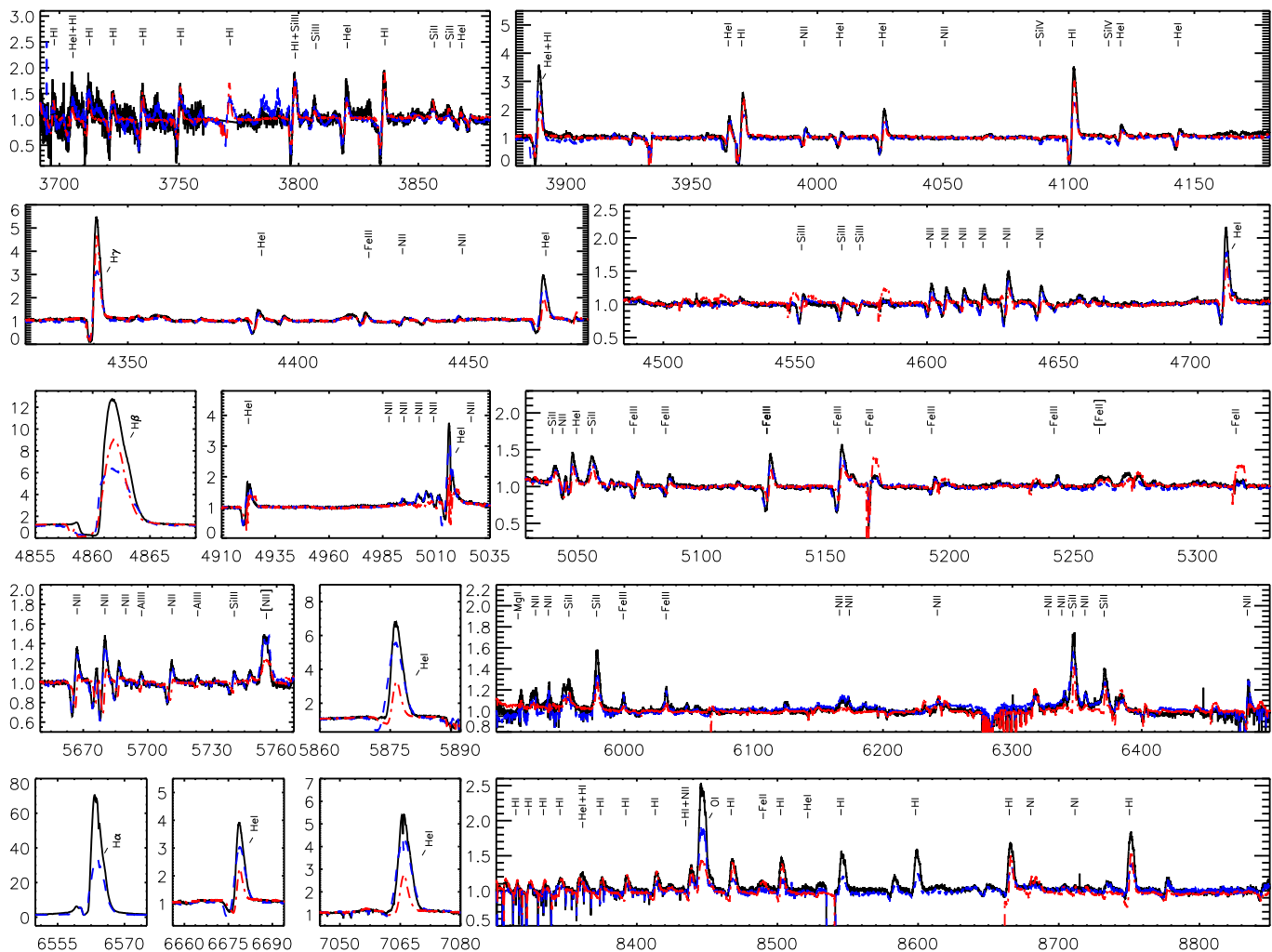


FIG. 3.— Evolution of the optical spectrum of AG Car in the region 3690–8850 Å during the 2000–2003 minimum (see text for discussion). The spectra were obtained in 2001 April (black solid line), 2002 March (blue dashed line), and 2003 January (red dot-dashed line). Data obtained from 2000 July until 2001 June show no significant variability. The spectrum from 2003 January has a small gap in wavelength coverage between 8540 – 8660 Å, while H $\alpha$  is saturated and not shown.

a hydrostatic structure, there might still be uncertainties in the density structure below the sonic point due to the proximity to the Eddington limit and the choice of  $M$ , rotation rate, and viewing angle.

CMFGEN allows for the presence of clumping within the wind using a volume-filling factor approach. The wind is assumed to be homogenous close to the star, become partially clumpy at a characteristic velocity scale  $v_c$ , and achieves full clumpiness, with a volume-filling factor  $f$ , at large distances, as follows:

$$f(r) = f + (1 - f) \exp[-v(r)/v_c] . \quad (1)$$

Full line blanketing is included consistently in CMFGEN through the concept of superlevels, which groups similar energy levels into one single superlevel to be accounted for in the statistical equilibrium equations. In the analysis of AG Car, our initial atomic model consisted of H, He, C, N, O, and Fe in order to constrain the parameter regime to be explored. For the final modeling we included additional elements and ionization stages. The atomic models adopted for the final modeling are summarized in Table 3, and included H, He, C, N, O,

Na, Mg, Al, Si, Cr, Mn, Fe, Co, and Ni.

The synthetic spectra of AG Car presented in this paper were computed using CMF\_FLUX (Hillier & Miller 1998; Busche & Hillier 2005) and did not include effects due to rotation. As discussed in Busche & Hillier (2005), rotation mainly affects spectral lines formed close to the photosphere. Specifically in the case of AG Car during minimum, only Si IV and He II lines have their profile significantly changed by rotation (Groh et al. 2006; Paper II).

## 5. DISTANCE AND SYSTEMIC VELOCITY

The spectroscopic analysis using CMFGEN cannot constrain the distance to AG Car. Throughout this work, we assume that AG Car is located at  $d = 6$  kpc (Humphreys et al. 1989; Hoekzema et al. 1992).

Stahl et al. (2001) re-determined the heliocentric systemic velocity of AG Car and found  $v_{\text{sys}} = 10 \pm 5 \text{ km s}^{-1}$ , suggesting a lower kinematical distance in the range of 5–6 kpc, instead of a kinematical distance of 6.0–6.5 kpc

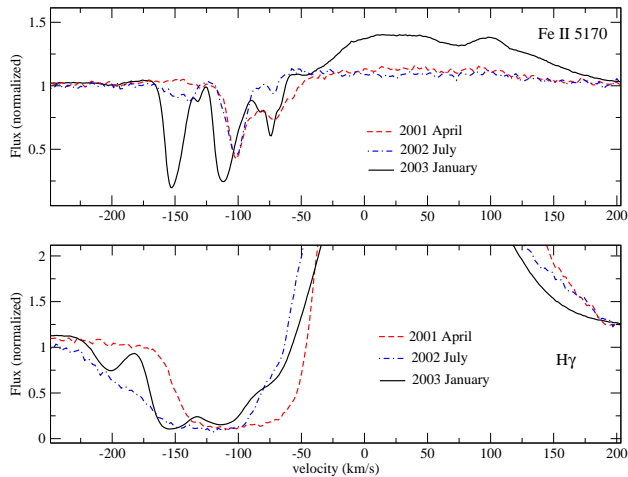


FIG. 4.— Evolution of the multiple absorption components seen in the AG Car spectrum during the minimum of 2000–2003. To illustrate their general behavior, we display the Fe II 5170 Å line (top) and H $\gamma$  4340 Å (bottom). The high-velocity multiple absorption components are likely caused by time-dependent effects, while the  $-72 \text{ km s}^{-1}$  component may also be formed in the circumstellar nebula of AG Car, which has an expansion velocity of  $\sim 70 \text{ km s}^{-1}$  (Nota et al. 1992).

from Humphreys et al. 1989<sup>9</sup>. Taking the errors into account, both determinations are consistent (Stahl et al. 2001). We also measured the centroid of the [Fe II] and [N II] lines in our high-resolution data and obtained  $v_{\text{sys}}$  similar to the value found by Stahl et al. (2001).

A note of caution regarding the kinematical distance of early-type stars should be pointed out: the distance to young stellar clusters based on spectroscopic parallax are systematically lower than their kinematical distance (e.g., Blum et al. 2000, 2001; Figuerêdo et al. 2002, 2008). In addition, about 10–30 % of Galactic O-type stars are runaways (Gies 1987; de Wit et al. 2005), implying that their derived kinematical distance might be meaningless. However, in the case of AG Car, the empirical luminosity-amplitude relationship found for LBVs (Wolf 1989) and the distance versus reddening relationship of nearby stars both support a distance of 6 kpc (Humphreys et al. 1989).

The bolometric luminosity  $L_{\star}$ , stellar radius  $R_{\star}$ , and mass-loss rate  $\dot{M}$  obtained through the spectroscopic analysis are distance-dependent, while the effective temperature and chemical abundances are only weakly, if at all, dependent on  $d$ . Following Schmutz et al. (1989), Najjarro et al. (1997), and Hillier et al. (1998), the physical parameters of AG Car obtained in this work (see Sect. 6) should be scaled to other distances according to:  $L_{\star} \propto d^2$ ,  $\dot{M} \propto d^{1.5}$ ,  $R_{\star} \propto d$ , and  $T_{\text{eff}} \propto d^0$ .

## 6. RESULTS

### 6.1. Surface chemical abundances

The surface chemical abundances obtained for AG Car are listed in Table 4. The values obtained are consistent when comparing different epochs from both minima, supporting the physical parameters derived for those epochs

<sup>9</sup> We updated the values of the kinematical distance presented by Humphreys et al. (1989),  $d_{\text{kin}} \simeq 6.4 - 6.9$  kpc, in order to account for a revised galactocentric distance of the Sun of  $R_0 = 8$  kpc and  $\Theta_0 = 220 \text{ km s}^{-1}$ , obtaining  $d_{\text{kin}} \simeq 6.0 - 6.5$  kpc, depending on whether the Galactic rotation curve of Fich et al. (1989) or Brand & Blitz (1993) was chosen.

TABLE 3  
FINAL ATOMIC MODEL USED  
IN THE ANALYSIS OF  
AG CAR

Ion	$N_S$	$N_F$	$N_T$
H I	20	30	435
He I	40	45	233
He II	22	30	435
C II	16	54	366
C III	30	54	268
C IV	21	64	1446
N I	44	104	885
N II	41	84	530
N III	30	63	344
O I	69	161	358
O II	19	57	372
O III	17	79	450
Na I	22	71	1550
Mg II	18	45	358
Al II	21	65	1348
Si II	22	43	182
Si III	20	34	92
Si IV	22	33	183
Cr II	42	310	2127
Cr III	40	209	4077
Cr IV	29	234	4466
Cr V	30	223	3207
Mn II	33	333	1348
Mn III	33	333	4038
Mn IV	39	464	11103
Mn V	16	80	676
Fe II	61	261	3837
Fe III	33	191	6935
Fe IV	58	383	2816
Fe V	25	168	1938
Co II	54	421	3267
Co III	22	174	3837
Ni II	29	204	4728
Ni III	28	220	5181
Ni IV	36	200	2337
Ni V	46	183	1524

NOTE. — For each species, an additional one-level ion corresponding to the highest ionization stage was included explicitly in the rate equations (i.e. C V for carbon, for instance), but are not shown above for brevity. The columns correspond to the number of included superlevels ( $N_S$ ), total energy levels ( $N_F$ ), and the number of bound-bound transitions included for each ion ( $N_T$ ).

(Sect. 6.2 and 6.3).

The helium abundance of AG Car was determined as  $\text{He}/\text{H} = 0.43 \pm 0.08$  (in number) in order to reproduce the intensity of He I, He II and hydrogen lines in the optical and near infrared spectrum. This value is in agreement with previous works (Smith et al. 1994; Leitherer et al. 1994; Stahl et al. 2001), and with the helium content for the LBV phase predicted by evolutionary models (Meynet & Maeder 2000). Unlike Eta Carinae (Hillier et al. 2001) and HD 316285 (Hillier et al. 1998), the deduced helium abundance of AG Car does not scale with the derived mass-loss rate. This is because AG Car simultaneously presents He I and He II lines in the spectrum during minimum, while Eta Car and HD 316285 do not.



In addition to the helium content, it is essential to determine the abundance of the CNO-elements to constrain the evolutionary stage of AG Car. A nitrogen mass fraction of  $(7.2 \pm 2) \times 10^{-3}$  ( $11.5 \pm 3.4$  times the solar value; hereafter, we used the solar abundance values listed in Grevesse et al. 2007 and references therein) was obtained based on numerous N II lines in the optical spectrum (4601–4643, 6482 Å) and on ultraviolet N III lines. The carbon abundance was determined based on the strength of optical C II lines at 6578–6582 Å and 7231–36 Å, yielding a carbon mass fraction of  $(2.4 \pm 0.7) \times 10^{-4}$  ( $0.11 \pm 0.03$  times the solar value). The errors in the carbon and nitrogen abundance are about 30%. The oxygen mass fraction was determined to be  $(2.4 \pm 1) \times 10^{-4}$  ( $0.04 \pm 0.02$  times the solar value) using the O I lines at 7774–8446 Å and O II 4620 Å. As it was not possible to fit both O I lines with the same model, the uncertainty in the oxygen abundance is around 50%. Nonetheless, it is safe to point out that the oxygen abundance on the surface is very low compared to the solar value. Together with the high nitrogen content and carbon depletion, we conclude that there is certainly CNO-processed material on the surface of AG Car. The total C+N+O abundance of AG Car is in broad agreement with a solar composition.

The CNO cycle is also supposed to enhance the Na abundance in massive stars by a factor of  $\sim 4$  (Prantzos et al. 1986), which could be investigated using the wind component of the optical resonance lines of Na I 5885–5890 Å. We found that Na is overabundant by a factor of  $3.3 \pm 1$  in comparison to the solar value.

The rich emission-line spectra of AG Car also allowed us to constrain the Si and Mg surface abundances. The former was obtained using the ultraviolet and optical lines of Si II, Si III, and Si IV, while the latter was constrained using Mg II lines at 4481, 10915, and 10952 Å. For both species, the derived abundance is consistent with the solar value within 30%.

Iron contributes significantly to the emergent spectrum of AG Car and, together with other iron-group elements, is the main responsible for the severe line blanketing seen in the ultraviolet spectrum. Solar abundance was initially assumed for Fe, Ni, Cr, Mn, and Co, and was found to be consistent with the line blanketing seen in the UV. The severe line blending with Fe lines and uncertainties in the atomic parameters make it impossible to constrain the Ni, Cr, Mn, and Co abundance better than a factor of 2. The Fe content can be better constrained to within  $\pm 30\%$  of the solar value using the numerous Fe II and [Fe II] lines in the optical spectrum and the Fe II forest in the ultraviolet.

## 6.2. Stellar and wind parameters during the 1985–1990 minimum

We divided the data obtained from 1985–1990 into three subsets which were analyzed separately as follows. The first epoch comprised spectra from 1985 July until 1986 June, since the H $\alpha$  spectrum obtained in 1986 June showed significantly enhanced emission compared to other epochs (Fig. 2). In the second subset, the data from 1987 January until 1990 June were averaged and analyzed as a single-epoch observation, since very little variability was present. We believe that the fundamental parameters obtained during these epochs are the least

TABLE 4  
SURFACE CHEMICAL ABUNDANCES OF AG CAR

Species	Number fraction	Mass fraction	Z/Z $_{\odot}$ <sup>a</sup>
H	1.00	$3.6 \times 10^{-1}$	$0.49 \pm 0.05$
He	0.43	$6.2 \times 10^{-1}$	$2.5 \pm 0.2$
C	$5.6 \times 10^{-5}$	$2.4 \times 10^{-4}$	$0.11 \pm 0.03$
N	$1.4 \times 10^{-3}$	$7.2 \times 10^{-3}$	$11.5 \pm 3.4$
O	$4.1 \times 10^{-5}$	$2.4 \times 10^{-4}$	$0.04 \pm 0.02$
Na	$1.0 \times 10^{-5}$	$8.4 \times 10^{-5}$	$3.3 \pm 1$
Mg	$7.3 \times 10^{-5}$	$6.5 \times 10^{-4}$	$1.0 \pm 0.3$
Al	$5.7 \times 10^{-6}$	$5.6 \times 10^{-5}$	$1.0 \pm 0.3$
Si	$6.5 \times 10^{-5}$	$6.6 \times 10^{-4}$	$1.0 \pm 0.3$
Cr	$9.0 \times 10^{-7}$	$1.7 \times 10^{-5}$	$1.0^{+1}_{-0.5}$
Mn	$4.7 \times 10^{-7}$	$9.4 \times 10^{-6}$	$1.0^{+1}_{-0.5}$
Fe	$6.7 \times 10^{-5}$	$1.4 \times 10^{-3}$	$1.0 \pm 0.3$
Co	$1.6 \times 10^{-7}$	$3.5 \times 10^{-6}$	$1.0^{+1}_{-0.5}$
Ni	$3.4 \times 10^{-6}$	$7.3 \times 10^{-5}$	$1.0^{+1}_{-0.5}$

<sup>a</sup> Ratio between the mass fraction of a given species in AG Car and the respective solar mass fraction. Quoted errors indicate the range of abundances consistent with the observations. Solar abundances are from Grevesse et al. (2007).

affected by time-dependent effects. The third subset consisted of data from 1990 December until 1991 January, since the He II 4686 Å emission was noticeably weaker than other epochs during this minimum (Fig. 2).

Figures 5, 6, and 7 show the comparison between the best CMFGEN models obtained for the 1985–1990 minimum phase and the ultraviolet, optical, and near-infrared spectra of AG Car. The models quantitatively reproduce the observed spectrum with a superb fit in most spectral regions, in particular in the ultraviolet, where the line blending and blanketing are severe.

Table 5 presents the fundamental parameters of AG Car during the 1985–1990 minimum, and below we discuss the diagnostics used to derive each of them.

### 6.2.1. Effective temperature ( $T_{\text{eff}}$ ) and temperature at the base of the wind ( $T_{\star}$ )

During this minimum, the most sensitive diagnostic for deriving  $T_{\text{eff}}$  was the ratio between He II 4686 Å and He I lines at 4471 Å, 4713 Å, 5876 Å, 6678 Å, and 10024 Å. Changes of a few hundred K in  $T_{\text{eff}}$  were sufficient to change the EW of He II 4686 Å by a factor of 2. In addition, the ionization structure of C, N, and Si were also sensitive to  $T_{\text{eff}}$  and yielded similar values to  $T_{\text{eff}}$ . For the C ionization structure, we used the ultraviolet C II 1331–1334 Å, C III 1175 Å, and C III 1247 Å and the optical C II 6578–6582 Å and C II 7231–7236 Å diagnostic lines. In the case of the N ionization structure, we compared the strength of several optical N II lines such as N II 4601–07–30–43 Å, N II 6482 Å, and N II 6613 Å with the N III triplet at 1747–1749–1751 Å. The absence of N III lines around 4500 Å was used to constrain the maximum value of  $T_{\text{eff}}$  during 1987–1990. The Si ionization structure was constrained through the relative strength of Si II, Si III, and Si IV lines, using lines of Si II 6347 Å, Si III 1280–1290 Å, Si III 4553–4568–4575 Å, Si IV 1393–1402 Å, and Si IV 4088–4116 Å.

Using such a large number of relatively high-sensitive diagnostics available for  $T_{\text{eff}}$ , we obtained  $T_{\text{eff}} \simeq 22,800 \pm 500$  K during 1987–1990. There was no evidence

from the 1985 July and 1986 June UV spectra that  $T_{\text{eff}}$  was higher than during 1987–1990 within the errors, and therefore we also adopted  $T_{\text{eff}} \simeq 22,800 \pm 500$  K for both epochs. Even if the He II 4686 Å emission was slightly weaker in 1990 June than in 1989 March (Fig. 2), changing  $T_{\text{eff}}$  by a few hundreds of K within the given error is sufficient to fit this line. Thus, for simplicity and due to the absence of other extremely sensitive diagnostic lines, we assume that  $T_{\text{eff}}$  was constant during 1987–1990. The smaller He II 4686 Å emission during 1990 December–1991 January, when AG Car was brightening, suggests that the effective temperature was approximately 1000 K lower at that epoch ( $T_{\text{eff}} \simeq 21,500 \pm 500$  K).

Since the photosphere of AG Car is extended, we found that  $T_{\text{eff}}$  depends on the derived value of  $\dot{M}$  (Sect. 6.2.2), wind velocity law (Sect. 6.2.3), and  $M$  ( $\sim 70 M_{\odot}$ , Paper II). In addition, we found that the velocity and density structure below the sonic point significantly affect the value of  $T_{\text{eff}}$ . In our best models, the velocity structure was iterated at depth in order to fulfill the momentum equation below the sonic point. Initial models, which assumed a fixed scale height across the extended atmosphere, yielded higher values of  $T_{\text{eff}}$  by up to  $\sim 1000$  K.

The value of  $T_{\star}$  is defined in this paper as the temperature of the hydrostatic core (i.e. at the base of the wind,  $R_{\star}$ ) where  $v = v_{\text{sonic}}/3$  (Sect. 4), and the difference between  $T_{\star}$  and  $T_{\text{eff}}$  of a given epoch is directly related to the extension of the atmosphere. We obtained  $T_{\star} = 26,200 \pm 500$  K during 1987 January – 1990 June and  $T_{\star} \simeq 24,640 \pm 500$  K during 1990 December–1991 January. Since we assumed that  $T_{\text{eff}}$  was constant from 1985 July–1990 June, the higher mass-loss rate of AG Car obtained from 1985 July–1986 June compared to 1987 January – 1990 June (see Sect. 6.2.2) implies that the atmosphere was more extended between 1985 July–1986 June. Therefore,  $T_{\star}$  was slightly higher between 1985 July–1986 June ( $T_{\star} \simeq 26,450 \pm 500$  K) than during 1987 January – 1990 June.

### 6.2.2. Mass-loss rate and wind clumping

The mass-loss rate was obtained by reproducing the intensity of the strongest lines in the observed spectrum of AG Car: namely, those of hydrogen, helium, and nitrogen. Using those diagnostics we obtained  $\dot{M} = 1.5 \times 10^{-5} M_{\odot} \text{yr}^{-1}$  during 1987–1990. Spectra from 1990 December–1991 January are also consistent with the same  $\dot{M}$ . Figure 8 illustrates the effects of wind clumping on selected spectral lines of AG Car, presenting CMFGEN models assuming different volume-filling factors but with the same value of  $\dot{M} f^{-0.5} = 4.7 \times 10^{-5} M_{\odot} \text{yr}^{-1}$  and, thus, equally reproducing the amount of H $\alpha$  emission. We derived a volume-filling factor of  $f = 0.1$  based on the strength of the electron-scattering wings of H $\alpha$ , H $\beta$ , H $\gamma$ , H $\delta$ , and He I 6678 Å.

Similar to what has been found for O-stars (Hillier et al. 2003; Bouret et al. 2003, 2005), we found that clumps must be created very deep in the wind, close to the sonic point (i.e.  $v_c \simeq 20 \text{ km s}^{-1}$ ), in order to reproduce the weak electron-scattering wings of He II 4686 Å. The presence of clumps very close to the stellar surface is in line with the latest polarimetric results by Davies et al. (2005, 2006, 2007, 2008).

The statistical error in  $\dot{M}$  when using a single spectral line, such as H $\alpha$ , as diagnostic is as small as 5%. However, taking into account that multiple lines need to be fitted, that additional parameters can also change the line strength and have their own errors, and the assumptions in the model (prescribed velocity law, steady-state, spherical-symmetric wind, etc.), we estimate that the uncertainty in  $\dot{M}$  amounts to 30%. We found that models assuming either  $f \leq 0.05$  or  $f \geq 0.25$  do not provide reasonable fits to the electron-scattering wings present in the AG Car spectrum (Fig. 8).

As shown in Sect. 3.1, moderate spectroscopic variability is seen during the minimum only in the H $\alpha$  profile obtained in 1986 June, which was  $\sim 20\%$  stronger than during the rest of the minimum (1987–1990). To investigate the nature of the changes seen in H $\alpha$  and explain the behavior of AG Car during 1985–1990, we explored the parameter space around the best CMFGEN radiative transfer model obtained for 1987–1990 (see Table 5). This model spectrum does not have a P-Cygni absorption component in H $\alpha$  and provides a nice fit to the H $\alpha$  profile from 1987 June – 1990 June.

We found that the H $\alpha$  emission in 1986 June can be explained by an increase of  $\sim 30\%$  in  $\dot{M}$  compared to the value obtained for the rest of the minimum ( $\dot{M} = 1.5 \times 10^{-5} M_{\odot} \text{yr}^{-1}$ , see Sect. 6.2.2), corresponding to  $\dot{M} = 1.9 \times 10^{-5} M_{\odot} \text{yr}^{-1}$ . However, increasing  $\dot{M}$  by 30% is not sufficient to change the H ionization structure and does not produce a weak P-Cygni absorption component. Furthermore, the change in  $\dot{M}$  by 30% in the model produces a modest 1% increase in the  $y$ -band flux, or 0.01 mag. Interestingly, such an amount of photometric variability induced by the change in  $\dot{M}$  is compatible with the microvariability detected in AG Car during minimum (van Genderen et al. 1988, 1990).

As has been suggested in order to explain the spectroscopic changes seen in the LBVs He 3-519 (Crowther 1997) and P Cygni (Pauldrach & Puls 1990; Najjarro et al. 1997), we also found that the H ionization structure of AG Car could be affected by changes in  $\dot{M}$ ,  $R_{\star}$ , and  $L_{\star}$ . However, in the parameter regime found during 1985–1990, we determined that even if  $\dot{M}$  is increased by a relatively large factor of 4, the model spectrum does not show a weak P-Cygni absorption component, as seen in the observations. Therefore, a decrease in  $T_{\text{eff}}$  and/or  $L_{\star}$  is required in order to fit the weak P-Cygni absorption in the 1986 June spectrum. The decrease in  $T_{\text{eff}}$  is not supported by the ultraviolet spectrum taken in 1985–1990, while the change in  $L_{\star}$  would produce, according to our models, significant photometric changes of at least  $\sim 0.5$  mag, which is not observed during 1985–1990.

### 6.2.3. Wind terminal velocity and velocity law

We used the maximum velocity of the saturated P-Cygni absorption component of the UV resonance lines<sup>10</sup> of C II 1334–1335 Å, Si IV 1393–1402 Å, and Mg II 2798–2810 Å as a diagnostic to derive the wind terminal velocity. In the case of C II 1334–1335 Å both lines are blended, and only the blue component was used. The determination of  $v_{\infty}$  from UV resonance lines is very

<sup>10</sup> The so-called  $v_{\text{black}}$ , see Prinja et al. (1990).

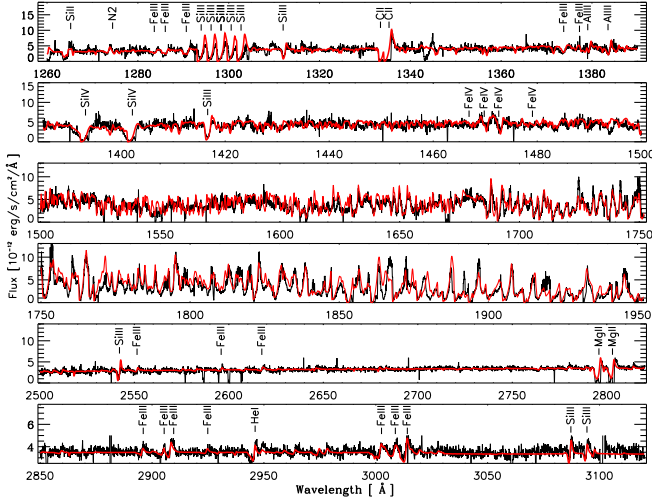


FIG. 5.— Comparison between the ultraviolet spectrum of AG Car from 1989 December 23 (black line) and the best CMFGEN model for that epoch reddened using  $E(B - V) = 0.65$  and  $R_V = 3.5$  (red line) in the spectral region between 1260 – 3150 Å. The same model provides similarly good fits to the other ultraviolet spectra of AG Car taken between 1985–1990, since there was little variability in the UV spectrum of AG Car during these epochs (Leitherer et al. 1994). Line identification for the strongest spectral features is presented. The spectrum in the region between 1500 – 1950 Å is highly blanketed and dominated by blends of Fe III, Fe IV, and Ni IV lines. Notice that Fe II lines are absent. The P III doublet lines at 1344.32–1344.85 Å were not included in the models.

weakly dependent on the assumed velocity law. Since the UV resonance lines essentially have no variability during minimum (Leitherer et al. 1994), all epochs between 1985–1989 yield  $v_\infty = 300 \pm 30 \text{ km s}^{-1}$ .

Additional constraints on the value of  $v_\infty$  can be obtained from the FWHM of the emission component of the strongest optical lines, such as H $\alpha$ , H $\beta$ , H $\gamma$ , and He I lines, and from the P-Cygni absorption profile of the He I lines. Using these diagnostics, we derived  $v_\infty = 270 \pm 50 \text{ km s}^{-1}$ , which is slightly lower but still in line with the value obtained from the UV resonance lines. The optical lines provided only a lower limit to  $v_\infty$ , since they were much more sensitive to the adopted velocity law and to the density structure of the wind than the UV resonance lines, which explains the different results comparing optical and UV analyses. Using only the optical lines, lower values of  $v_\infty$  were obtained when low values of the wind acceleration parameter  $\beta$  were used. In particular, a normal velocity law with  $\beta = 1$  would require  $v_\infty$  as low as  $230 \text{ km s}^{-1}$ , while higher values of  $\beta$  such as 3–4 would require a value of  $v_\infty$  closer to that obtained from the UV lines. Thus, ultimately, we favor the use of the value obtained from the UV lines,  $v_\infty = 300 \pm 30 \text{ km s}^{-1}$ , and that  $\beta$  is roughly 3. A high value of  $\beta$  is supported by several other diagnostics. Low values of beta did not simultaneously provide reasonable fits to UV resonance lines and to the optical H I and He I line profiles, in particular to their absorption profile. In addition, the ratio between H $\alpha$  and the other Balmer lines such as H $\beta$  and H $\gamma$  required  $\beta \geq 3$ . Values of  $\beta < 3$  also yielded too much radiative acceleration beyond the sonic point (Paper II).

Evidence of an extended acceleration zone in the outer wind is suggested by the wind hydrodynamics: a velocity

law using a single value of  $\beta$  yielded too much radiative acceleration for distances greater than  $\sim 10^2 R_*$  (Paper II). However, we chose to use a usual beta-type law in order to not introduce extra free parameters in the analysis.

Line-driven winds are intrinsically unstable, and turbulent motions are expected to arise (Owocki et al. 1988; Feldmeier 1995). Such a turbulent velocity field produces a non-saturated absorption wing extending to velocities higher than  $v_\infty$  on most UV resonance lines in the AG Car spectrum. In addition, a redshift of the emission components of the stronger H I, He I, and Fe II lines is also produced due to the turbulent velocity field (Hillier 1987, 1989; Catala et al. 1984). In CMFGEN, it is possible to account for a microturbulent velocity  $v_{\text{turb}}$ , which was set to  $20 \text{ km s}^{-1}$ . The use of higher values of  $v_{\text{turb}}$  causes a redshift of the emission component of the stronger He I and hydrogen lines, which is not seen in the observed spectrum. This also explains the shift of  $\sim +10 \text{ km s}^{-1}$  of the H $\alpha$  emission component, relative to the systemic velocity, measured by Stahl et al. (2001) (the same behavior is observed in our data). We obtained satisfactory fits to the extended, non-saturated absorption wing using  $v_{\text{turb}} = 20 \text{ km s}^{-1}$ .

Leitherer et al. (1994) noticed that during minimum the UV resonance lines of Si IV 1393–1402 Å have an extended, non-saturated absorption wing with velocities up to  $\sim -700 \text{ km s}^{-1}$ . Those authors interpreted this component either as evidence of a fast polar outflow of AG Car or as being caused due to blending with Fe lines (following Hubeny et al. 1985). Our models predict severe blending due to Fe III and Fe IV around both Si IV lines, which can mimic a high-velocity absorption wing. Therefore, we do not support the idea that the blueshifted, high-velocity component seen in the Si IV lines are actually due to a fast polar wind; instead, we support that they are caused by Fe III and Fe IV absorption lines. The high projected rotational velocity inferred for AG Car by Groh et al. (2006), and the inference that we are seeing AG Car close to edge-on, provides further evidence that the high-velocity absorption does not come from the polar wind.

### 6.3. Stellar and wind parameters during the 2000–2003 minimum

Unlike the previous minimum, the observations of AG Car between 2000–2003 show significant temporal variability. The data were divided in four datasets consisting of data between 2000 July–2001 June, 2002 March–2002 July, 2002 November, and 2003 January. There was little variability during the time intervals of 2000 July–2001 June and 2002 March–2002 July; therefore, the average spectrum was used for those intervals. As a consequence of the larger spectral coverage and higher spectral resolution, it was possible to use a larger number of optical diagnostic lines during 2000–2003 in comparison to the previous minimum. The spectra taken before 2000 July and after 2003 January indicate  $T_{\text{eff}} \leq 13,000 \text{ K}$ , constraining the duration of this minimum to at most 2.5 years. The maximum  $T_{\text{eff}}$  was only achieved during  $\sim 1$ –1.5 years (Table 5).

The absence of ultraviolet observations did not affect the determination of the stellar and wind parameters of

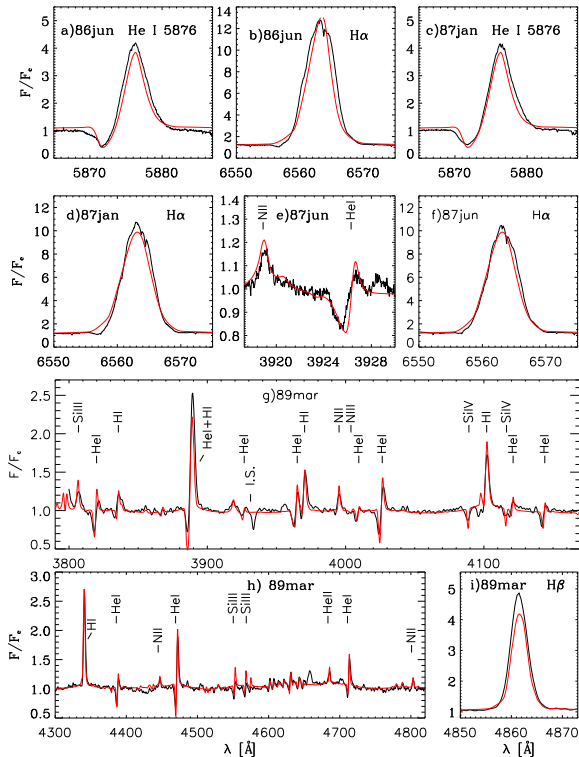


FIG. 6.— Optical spectra of AG Car taken at different epochs during the 1985–1990 minimum (black line) compared with the respective best CMFGEN model for each epoch (red line; see Table 5). Note the presence of [Fe III] 4658 Å during 1989 March in panel h.

AG Car since a much larger spectral coverage in the optical and near-IR was available compared to the 1985–1990 minimum, providing enough diagnostics. In addition, the main parameter obtained from ultraviolet lines, namely the wind terminal velocity, was determined based on the numerous P-Cygni absorption components of He I, N II, Fe II, and hydrogen Balmer and Paschen lines. For the data taken in 2001 May, it was also possible to constrain  $v_\infty$  using C III 1173 Å from the FUSE spectrum, yielding a similar value of  $v_\infty$  as the one found from the optical lines.

The optical diagnostic lines used to obtain the stellar and wind parameters are similar to those described in Sect. 6.2 and are just outlined here. The value of  $\dot{M}$  was obtained in order to reproduce the strength of the H, He, N, O, Mg, Si and Fe lines, while the volume-filling factor  $f$  was constrained using the intensity of the electron-scattering wings of the strongest H, He I, and Fe II lines.

The value of  $T_{\text{eff}}$  was determined based on the ionization structure of C, N, O, and Si, and on the relative strength between H and He I lines, assuming the He abundance obtained for the previous minimum. The presence of very weak He II 4686 Å emission was an additional constraint for the maximum value of  $T_{\text{eff}}$ . The N ionization structure was constrained by comparing the strength of numerous spectral lines<sup>11</sup> of N I (e.g., 7442,

<sup>11</sup> We refer to the atlas of Stahl et al. (1993) for a comprehensive identification of the spectral lines found in the parameter regime investigated in the present paper.

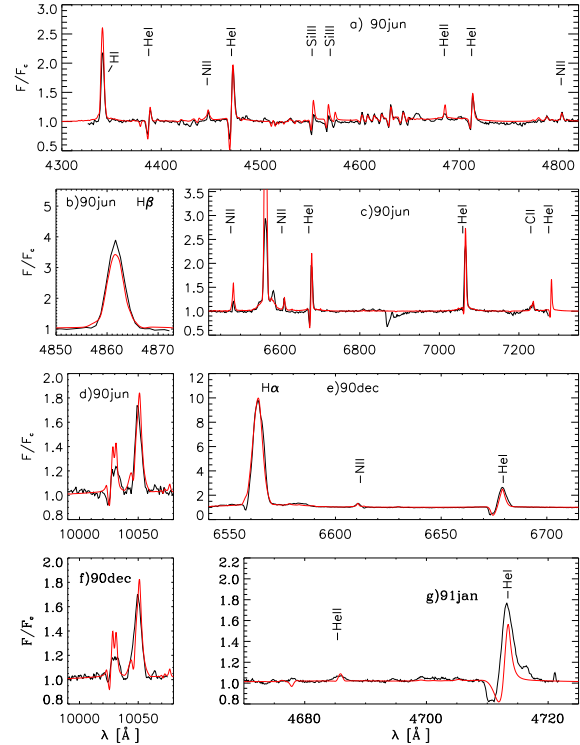


FIG. 7.— Optical and near-IR spectra of AG Car taken at different epochs during the 1985–1990 minimum (black line) compared with the respective best CMFGEN model for each epoch (red line; see Table 5). Notice in panel g that He II 4686 Å is broader in the observations than in the CMFGEN model, which is due to the fast rotation of AG Car (Groh et al. 2006; Paper II). In addition, the observed He I 4713 Å line profile is broader than the model in 1991 January (panel g).

7468, 8184–88, 8680–83–86, 8703–11–18 Å), N II (e.g., 4607–4630–4643, 6482 Å), and N III 4097 Å. Likewise, several O I (e.g. 8446 Å) and many weak O II lines (e.g., 3973, 4349, 4070–72, 4317–19–49, 4649 Å) present in the optical spectrum of AG Car were used to derive  $T_{\text{eff}}$ . Assuming the C abundance obtained for the previous minimum, the C ionization structure could be constrained based on the strength of several C II lines, such as those at 6578 – 82 Å and 7231 – 36 – 37 Å. Optical spectral lines of Si II, Si III, and Si IV were also used as diagnostics of  $T_{\text{eff}}$ . The values of  $T_{\text{eff}}$  provided by different diagnostics were consistent within  $\sim 500$  K.

The strength of Fe III and some Fe II lines were well reproduced by the CMFGEN models, supporting the value obtained for  $T_{\text{eff}}$  and  $\dot{M}$ . Note that a few Fe II lines, in particular those formed in the outer part of the wind such as Fe II 5169 Å, were stronger in the models than in the observations. We suspect that these lines are affected by time-dependent effects.

Figures 9a, 9b, and 9c present the observed AG Car spectra from 2001 April, 2002 March, and 2003 January, respectively, and the corresponding best CMFGEN model for each epoch. In general, a reasonably good fit to the observed spectrum could be obtained. However, in the 2001 April data a weak excess emission on top of the P-Cygni profile of H and He I is present approximately between +130 and +250 km s<sup>-1</sup>, and is not reproduced by the models. Such an excess emission could be caused

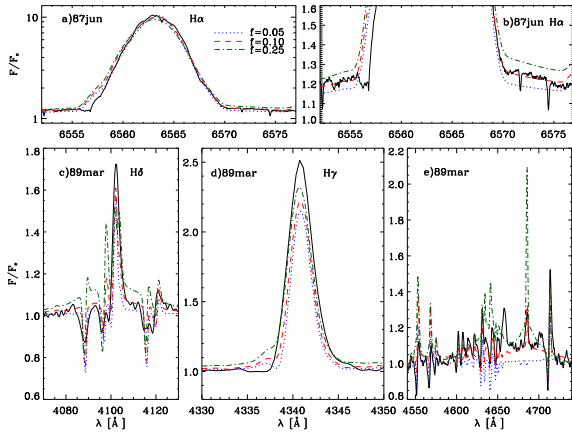


FIG. 8.— Optical spectra of AG Car taken at different epochs during the 1985–1990 minimum (black line) compared with CMFGEN models assuming different volume-filling factors  $f$  and with  $\dot{M}$  scaled to produce a similar amount of H $\alpha$  emission (i.e., all models have the same  $\dot{M}f^{-0.5} = 4.7 \times 10^{-5} M_{\odot}\text{yr}^{-1}$ ). For each epoch we display models with  $f = 0.05$  (dotted blue line),  $f = 0.10$  (dashed red line), and  $f = 0.25$  (dot-dashed green line). Notice that the model with  $f = 0.25$  produces too strong electron scattering wings and increased He II 4686 Å emission. Increasing the characteristic velocity at which clumps start to form ( $v_c$ ) from 20 to  $70 \text{ km s}^{-1}$  produces a similar effect to the He II 4686 Å emission as increasing the volume-filling factor, since this line is formed very deep in the wind. Note in panel c that the Si IV 4088 – 4116 Å absorptions are broader in the observations than in the CMFGEN model because rotational broadening was not included (Groh et al. 2006; Paper II).

by a latitude-dependent wind or by a velocity law different than the usual beta-type law assumed in this work. The values obtained for  $T_{\star}$ ,  $T_{\text{eff}}$ ,  $v_{\infty}$ ,  $\dot{M}$ , and  $f$  are listed in Table 5.

#### 6.4. The FUSE spectrum of AG Car and the extreme line blanketing in the far ultraviolet

Since the launching of the Far Ultraviolet Spectroscopic Explorer (FUSE) satellite, high-resolution far-ultraviolet spectroscopy of OB and WR stars has provided invaluable constraints on their fundamental properties, since a significant fraction of the stellar light is emitted in this spectral region and important diagnostic lines fall in the far ultraviolet. For a recent review on the accomplishments of the far-UV research of massive stars, see Crowther (2006).

Figure 10 shows the comparison between the archival FUSE spectrum of AG Car obtained during 2001 May and the best CMFGEN model for that epoch reddened using  $E(B - V) = 0.65$  and  $R_V = 3.5$  (see Sect. 6.5). The CMFGEN model spectrum matches reasonably well the observations, and the FUSE spectrum is consistent with the presence of a dense wind, indicating  $\dot{M}$  in the range  $3 - 4 \times 10^{-5} M_{\odot}\text{yr}^{-1}$ . The relative strength of Fe II and Fe III lines is the main diagnostic for  $T_{\text{eff}}$ , and agrees with the value derived from the optical/near-IR analysis. The many Fe II and Fe III transitions provide a good constraint on  $v_{\infty}$ , as does C III 1173 Å: all these diagnostics indicate a very low wind terminal velocity during 2001 May ( $v_{\infty} \simeq 90 - 130 \text{ km s}^{-1}$ ).

It can readily be noticed in Fig. 10 that line blanketing is extreme in the far-UV, and the determination of the continuum level with confidence is impossible from

the observations alone. Besides C III 1173 Å, the identification of other spectral features is hampered by the severe line overlapping present in the far-UV. In order to determine which species are responsible for a given spectral feature, we computed the observed spectrum due to a given ion using CMF\_FLUX (Busche & Hillier 2005). We found that most of the observed spectral features in the far-UV are actually a blend of line transitions, even in the case of C III 1173 Å, which is contaminated by Fe II and Fe III lines (Fig. 10). We present in Fig. 10 the separate contributions of lines of a given ion to the observed spectrum of AG Car. Most of the line blanketing in the FUSE range is provided by Fe III, while the contribution of other species are localized to a certain spectral range. In the 2001 spectrum of AG Car, most of the Fe II blanketing in the far-UV is in the spectral region 1050–1180 Å; Cr III contributes at 1000–1070 Å, Co III at 920–965 Å, and Ni III around 950–980 Å.

As has been seen in Galactic OB-type stars (Pellerin et al. 2002), the interstellar absorption due to H and H<sub>2</sub> significantly affects the observed spectrum below 1100 Å. A direct visualization of the influence of the interstellar absorption on the spectrum can be seen by comparing similar stars in the Galaxy (Pellerin et al. 2002) and the Magellanic Clouds (Walborn et al. 2002). In order to illustrate this effect for AG Car we also display on Fig. 10 the model spectrum taking into account the interstellar absorption by H and H<sub>2</sub>, using a procedure described by Herald et al. (2001), and assuming  $\log[N(\text{H}) \text{ cm}^2] = 21.0$  and  $\log[N(\text{H}_2) \text{ cm}^2] = 21.0$ . It is beyond the scope of this work to provide a detailed analysis of the interstellar spectrum towards AG Car.

#### 6.5. Luminosity, bolometric correction, and reddening

The luminosity of AG Car during the epochs presented in this paper was constrained by comparing the observed flux of each epoch (Table 1) with the reddened flux predicted by the CMFGEN model (Fig. 11). For the minimum phase of 1985–1990, we used observations from the ultraviolet (1200 Å) to the near-infrared ( $L$  band), while for the 2000–2003 minimum, we had available photometry in the  $V$ ,  $J$ ,  $H$ ,  $K$ , and  $L$  bands. A sole far-ultraviolet flux-calibrated spectrum obtained in 2001 May was additionally used for this epoch. Note that no AAVSO observations were used to derive a  $V$ -band flux due to their relatively low accuracy compared to LTPV and ASAS-3 photoelectric observations.

We obtained a bolometric luminosity for AG Car of  $L_{\star} = 1.5 \times 10^6 L_{\odot}$  during 1985–1990 and 2000–2001, which is listed in Table 5 together with the other wind and stellar parameters. However, a lower luminosity of  $L_{\star} = 1.0 \times 10^6 L_{\odot}$  and  $L_{\star} = 1.1 \times 10^6 L_{\odot}$  was derived for the 2002 March–July and 2003 January observations, respectively. Figure 11 shows a clear trend towards lower luminosity during the end of the 2000–2003 minimum. Excluding errors in the distance, the typical error in  $L_{\star}$  solely from the spectroscopic analysis is around 10% (gray region in Fig. 11).

Because of our limited spectroscopic and photometric sample, the scope of this paper is to describe the long-term behavior of the stellar parameters of AG Car. Therefore, we did not attempt to obtain a different bolometric luminosity for epochs relatively close in time

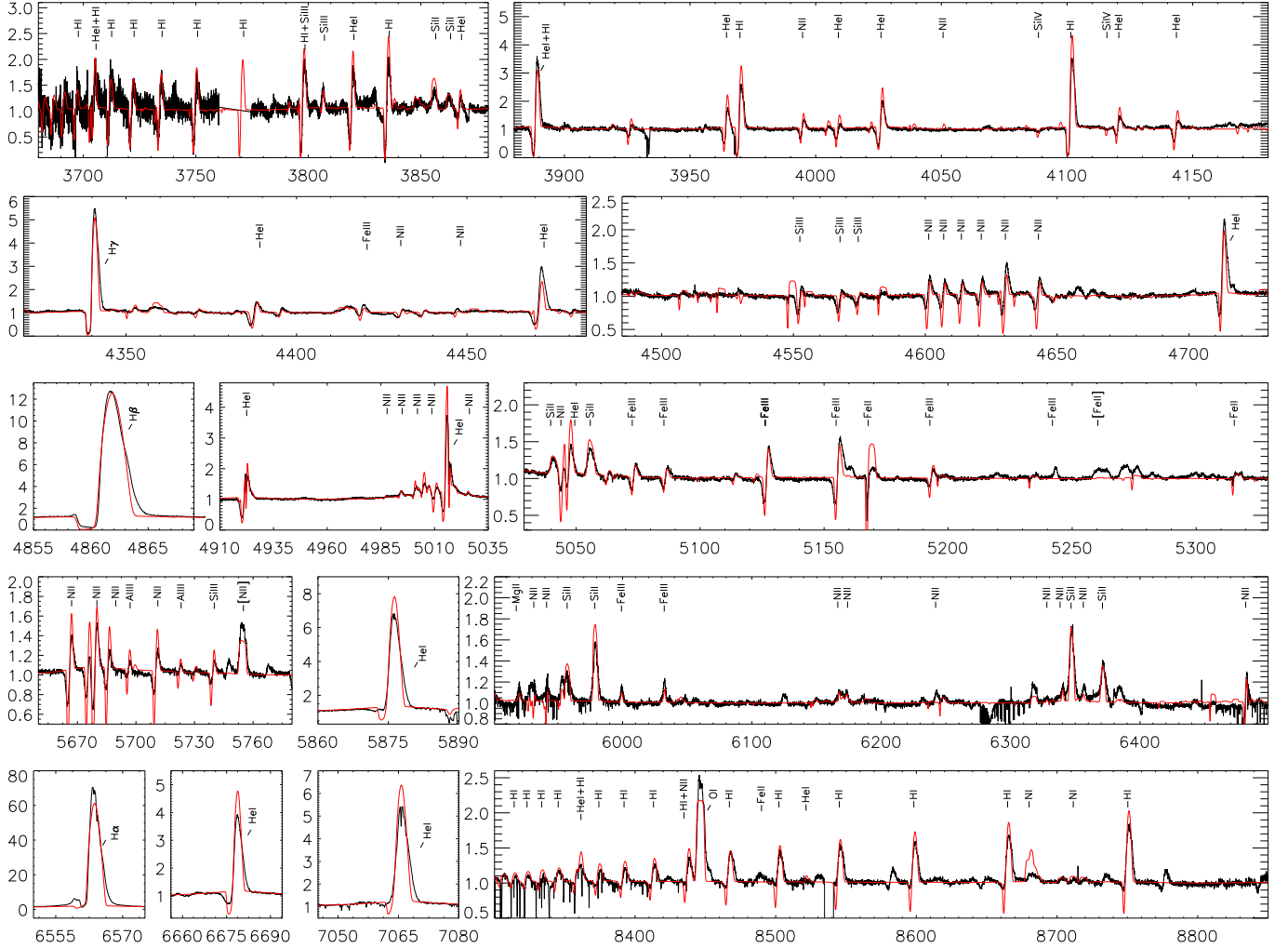


FIG. 9A.— Comparison between the observed spectrum of AG Car from 2001 April (black line) and the best model obtained with CMFGEN (red) in the spectral region between 3680–11000 Å. For all plots, the x-axis is the wavelength in Angstroms, while the y-axis represents the continuum-normalized flux. The identification of the stronger spectral lines is also shown [see the electronic version of the journal for fits to 2002 and 2003 data].

( $\Delta t \sim 3 - 6$  months), when little spectroscopic variability was seen. This was the case, for instance, for 1989 March–1989 December, 2001 April–2001 June, and 2002 March–2002 July. Although AG Car clearly presented photometric variability during these time periods, we assumed a constant bolometric luminosity for each of these periods and derived an average bolometric luminosity which, within the errors, could describe the SED during the whole time interval. Note that, according to Fig. 11, such an assumption does not change the main result of this Section, i.e., a lower bolometric luminosity as the star is moving towards maximum.

A much larger amount of spectroscopic and photometric data with a higher time sampling, together with a careful treatment of time-dependent effects in the radiative transfer model, are needed to study the behavior of the stellar parameters of LBVs on timescales of the order of a couple of months. Nevertheless, if the bolometric luminosity is variable on these short timescales, its amplitude is likely much smaller ( $\Delta \log[L_*/L_\odot] \sim 0.02$  dex) than the amplitude of the long-term variability ( $\Delta \log[L_*/L_\odot] \sim 0.17$  dex). Therefore, small fluctuations

of  $\pm 0.02$  dex in  $\log(L_*/L_\odot)$  may occur within each range of epochs shown Table 1, but such variations are within the errors of our modeling.

Since we derived  $L_*$  based on the comparison between the observed and model spectral energy distributions, different values of  $L_*$  could in principle be obtained by changing  $\dot{M}$  and  $T_{\text{eff}}$ . However, unrealistic changes in these parameters are required in order to reach the same value of  $L_*$  for all the different minimum epochs; for instance,  $T_{\text{eff}}$  would need to be reduced/increased by more than 2000 K for a given epoch, which is not supported by the line fits, in order to change the derived value of  $L_*$  by 30%. A similar drastic change in  $\dot{M}$  by more than a factor of 2, which again is not supported by the line fits, would be required in order to change the continuum emission and thus fit the data with the same  $L_*$  for all epochs. Even then, very peculiar reddening laws, which would be different for each epoch, would be required in order to reproduce the shape of the SED.

Therefore, the decrease in the bolometric luminosity obtained during the end of the minimum is robust, implying that the bolometric luminosity changes during the

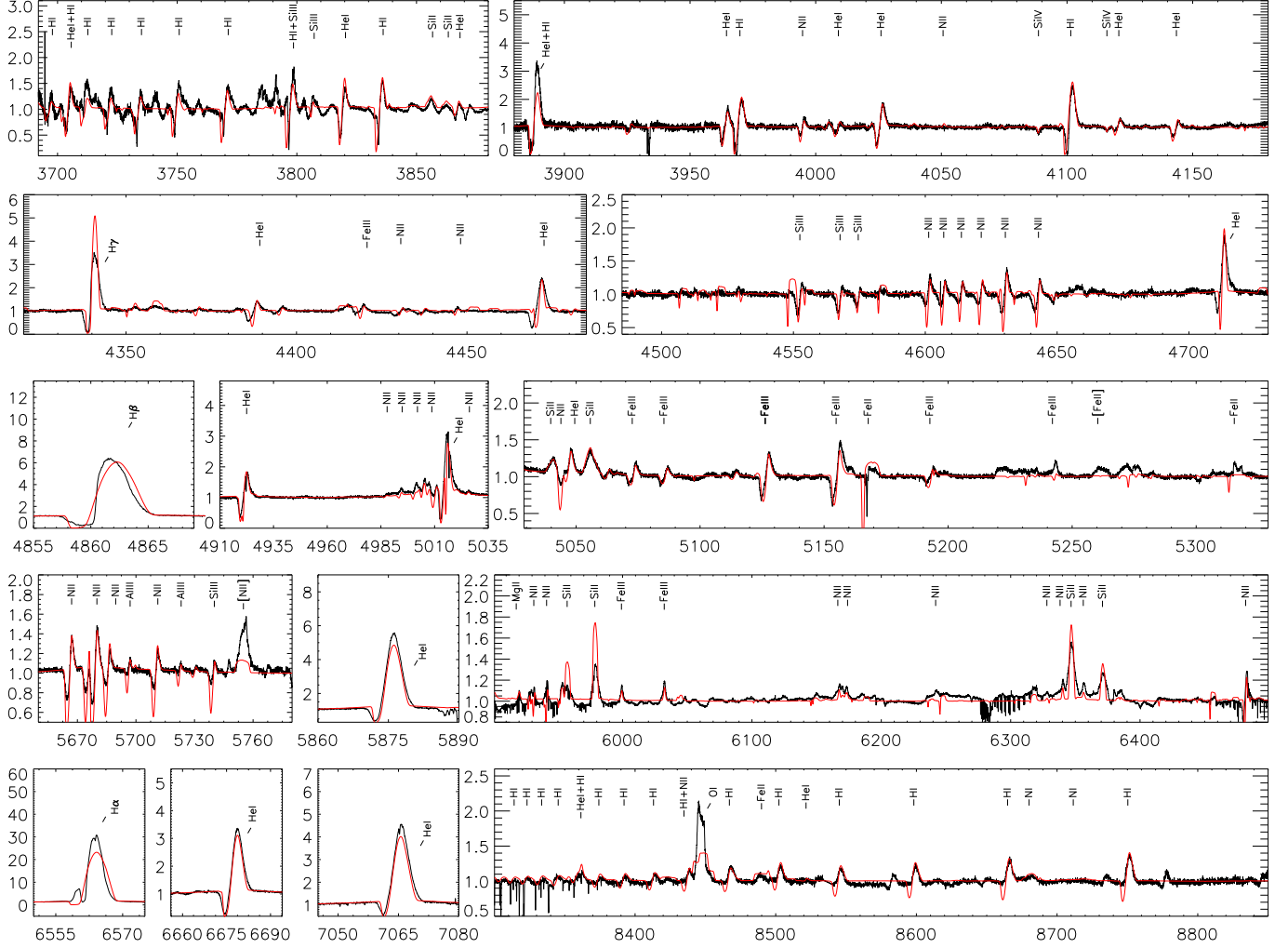


FIG. 9B.— Similar to Fig. 9a, but for data taken in 2002 March.

*S-Dor cycles of AG Car.* The similar maximum value of  $L_*$  derived for AG Car, for both minimum phases analyzed in this work, is indicative that this is the maximum luminosity of AG Car during minimum. On the other hand, the change in bolometric luminosity is contrary to the currently widely accepted paradigm of S-Dor variability at constant  $L_*$ . A detailed analysis of the changes of  $L_*$  during the full S-Dor cycle will be presented in Paper III.

The bolometric correction ( $BC$ ) in the V-band for each epoch was also obtained from our modeling and is presented in Table 5. As a consequence of the different stellar parameters, the  $BC$  of AG Car is also different in consecutive minima, ranging from  $\simeq -2.50$  mag (1985–1990) to  $-2.15$  mag (2000 July–2001 June). Further change in  $BC$  occurs when AG Car is moving towards maximum ( $BC \simeq -1.68$  mag during 2002 March–July and  $BC \simeq -1.22$  mag in 2003 January).

While it is well known that the bolometric correction of stars which have a negligible wind (such as the Sun and OB stars) is dependent on  $T_{\text{eff}}$  and  $\log g$ , we found that the bolometric correction of LBVs, because of the atmospheric extension, is dependent not only on  $T_{\text{eff}}$  and  $\log g$  but also on the wind density (and thus on  $\dot{M}$  and/or

$v_\infty$ ). Since  $T_{\text{eff}}$  also depends on the wind density, LBVs with different stellar parameters can have a similar value of  $T_{\text{eff}}$  but significantly different BCs; this is exactly the case for AG Car during 2001 April and 2002 March (see Table 5). While  $T_{\text{eff}}$  was close to  $\sim 17,000$  K during both epochs, the star was very different at depth, as can be readily evidenced by the very different temperatures at the hydrostatic radius in 2001 April ( $T_* \simeq 21,900$  K) and 2002 March ( $T_* \simeq 18,700$  K). Therefore, the BCs were different, and the effective temperature was similar just by coincidence. A complete analysis of the bolometric correction of LBVs over a broad range of physical parameters is beyond the scope of this work, and will be presented elsewhere.

Together with  $L_*$ , the reddening law towards AG Car was obtained through the comparison of the observed flux and CMFGEN models reddened according to the law of Fitzpatrick (1999). The best fits were obtained using  $E(B - V) = 0.65 \pm 0.01$  and  $R_V = 3.5 \pm 0.1$ , and are shown in Figure 11. Taking the uncertainties into account, it was possible to fit the data from both minima with the same reddening law, corroborating the physical parameters obtained for both epochs. The value of  $E(B - V) = 0.65$  is only slightly higher than previous

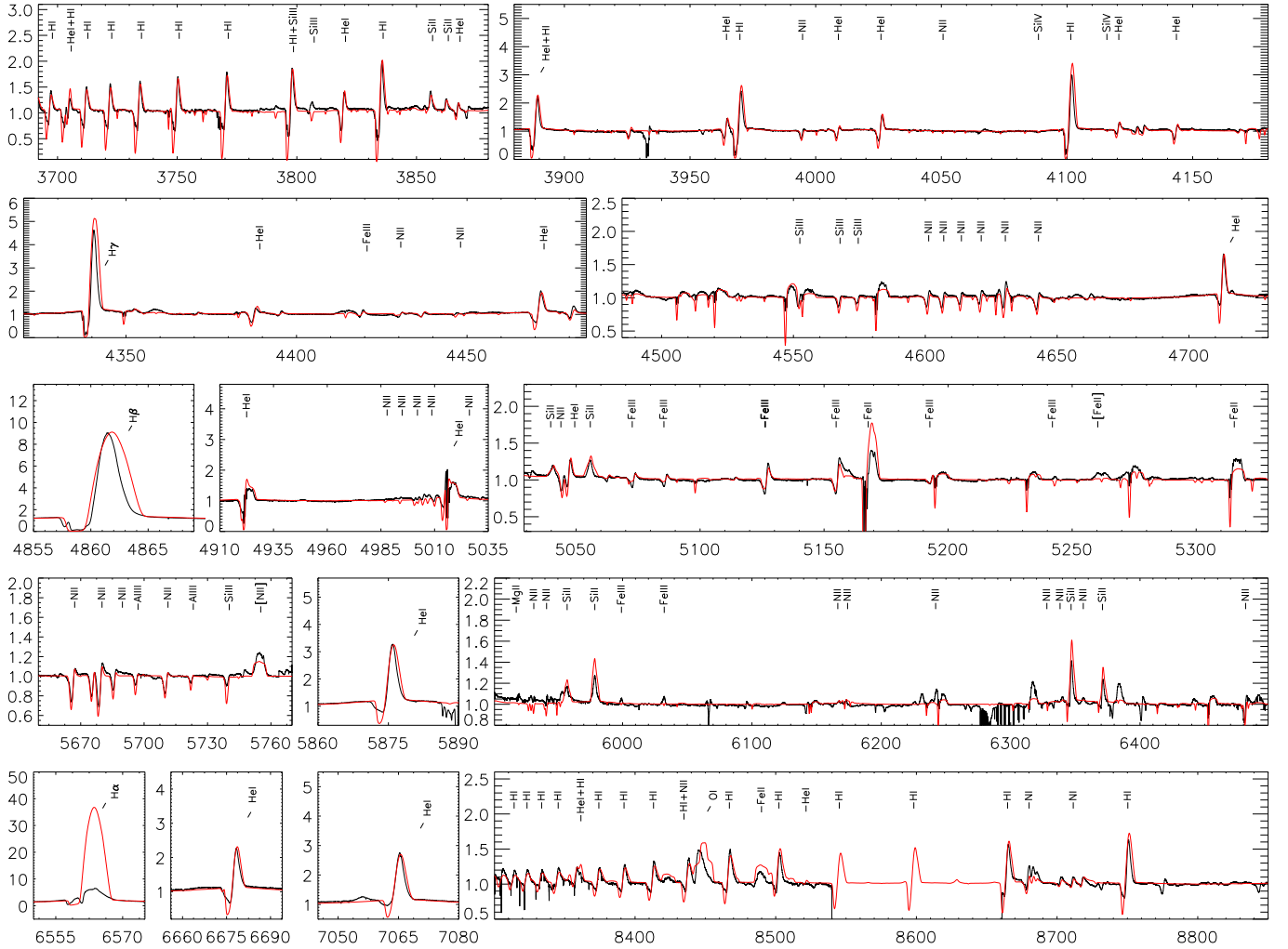


FIG. 9c.— Similar to Fig. 9a, but for data taken in 2003 January. Note that H $\alpha$  is saturated and was not used as a diagnostic.

determinations ( $E(B - V) = 0.63$ ) obtained using simple models and assuming constant bolometric luminosity (Humphreys et al. 1989; Shore et al. 1996).

Although the value of  $R_V = 3.5$  obtained in this work is higher than the standard value due to diffuse dust ( $R_V = 3.1$ ), it is lower than  $R_V = 3.9$ , as suggested by Schulte-Ladbeck et al. (1994) and based on the analysis of the polarimetric data of AG Car. Our results are compatible with the presence of large grains ( $\sim 1\mu\text{m}$ ) in the circumstellar environment of AG Car (Hyland & Robinson 1991), and with the very low amount of nebular reddening which has been inferred ( $A_V \sim 0.025 - 0.05$ , McGregor et al. 1988a).

The agreement between the CMFGEN models and the observed SED of AG Car from the far-ultraviolet to the  $L$ -band is superb. The free-free emission of the wind predicted by the CMFGEN models agrees very well with the observed SED in the near-IR, suggesting that the amount of warm and hot dust ( $\sim 800\text{--}1500\text{ K}$ ) present in the close vicinity of AG Car ( $1\text{--}2''$ ) is negligible.

## 7. DISCUSSION

### 7.1. Chemical abundances on the surface of AG Car and on the bipolar nebula

The chemical abundance on the surface of AG Car, presented in Table 4, clearly shows enhancement of He, N, and Na, together with a depletion of H, C, and O compared to the solar value, which is a fingerprint that CNO-processed material is present on the stellar surface and wind of AG Car. Since AG Car is a prototype of the LBV class, the abundances obtained in this work quantitatively confirm the prediction that LBVs have material processed by the CNO-cycle and significant He enrichment on their surfaces (see e.g. Humphreys & Davidson 1994, Crowther 1997), which put tight constraints on their evolution.

Table 6 presents the abundances obtained in this work for the surface of AG Car and the available nebular values. Their comparison might provide clues to the evolution of AG Car during the LBV phase, since the nebula was ejected  $\sim 10^4$  years ago (Smith et al. 1997; Lamers et al. 2001). Unfortunately, nebular abundances are only reliable for N and O, since the He and C lines are weak or absent in the nebular spectrum (Mitra & Dufour 1990; de Freitas Pacheco et al. 1992; Nota et al. 1992; Smith et al. 1997). The He abundance was estimated by Lamers et al. (2001) based on several evolutionary assumptions and on the ratio N/O obtained for the nebula.



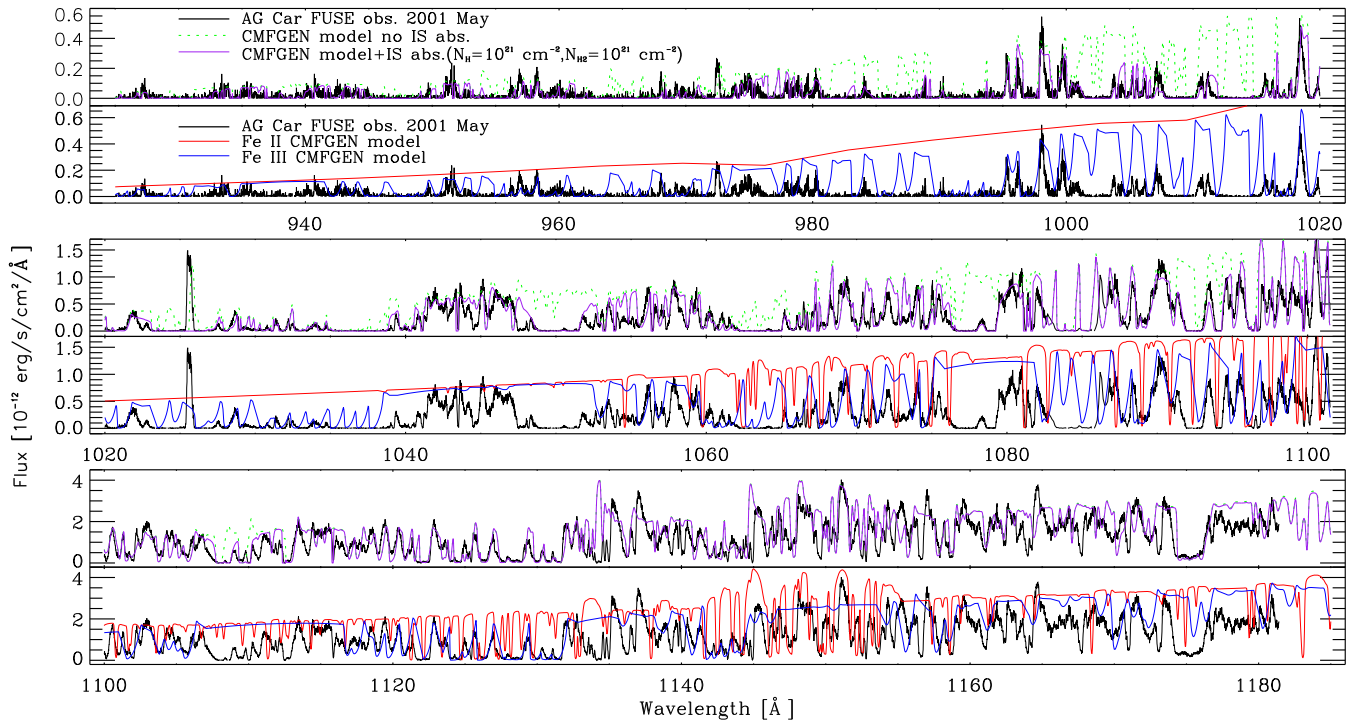


FIG. 10.— Far-ultraviolet spectrum of AG Car observed with FUSE in 2001 May (black solid line) compared with the best CMFGEN model for this epoch (green dotted line), reddened using  $E(B - V) = 0.65$  and  $R_V = 3.5$ . The CMFGEN model was scaled in flux in order to better match the continuum level. The best model, taking into account an interstellar absorption spectrum due to H I with  $\log[N(\text{H}) \text{ cm}^2] = 21.0$  and  $\text{H}_2$  with  $\log[N(\text{H}_2) \text{ cm}^2] = 21.0$ , is shown in order to infer the influence of those transitions on the morphology of the far-ultraviolet spectrum of AG Car (purple solid line). For each wavelength range, the bottom panel shows the best CMFGEN model spectrum computed including continuum emission and bound-bound transitions due to only Fe II (red solid line) or only Fe III (blue solid line), in order to facilitate line identification. These ions are the main contributors to the line blanketing in the far-UV and illustrate how well CMFGEN can handle the effects caused by the extreme blending due to tens of spectral lines.

TABLE 5  
STELLAR AND WIND PARAMETERS OF AG CAR DURING MINIMUM EPOCHS

Epoch	$V^a$	BC (mag)	$\log(L_*/L_\odot)^b$ (mag)	$R_*$ ( $R_\odot$ )	$R_{\text{phot}}$ ( $R_\odot$ )	$T_*$ (K)	$T_{\text{eff}}$ (K)	$\dot{M}$ ( $M_\odot \text{ yr}^{-1}$ )	$v_\infty$ ( $\text{km s}^{-1}$ )	f
1985 Jul – 1986 Jun	7.98	-2.50	6.17	58.5	78.7	26,450	22,800	$1.9 \times 10^{-5}$	300	0.10
1987 Jan – 1990 Jun	8.00	-2.52	6.17	59.6	78.7	26,200	22,800	$1.5 \times 10^{-5}$	300	0.10
1990 Dec – 1991 Jan	7.71	-2.23	6.17	67.4	88.5	24,640	21,500	$1.5 \times 10^{-5}$	300	0.10
2000 Jul–2001 Jun	7.63	-2.15	6.17	85.3	141.6	21,900	17,000	$3.7 \times 10^{-5}$	105	0.15
2002 Mar–2002 Jul	7.60	-1.68	6.00	95.5	124.2	18,700	16,400	$4.7 \times 10^{-5}$	195	0.25
2002 Nov	7.20	-1.28	6.00	120.4	170.4	16,650	14,000	$6.0 \times 10^{-5}$	200	0.25
2003 Jan	7.03	-1.22	6.04	115.2	171.3	17,420	14,300	$6.0 \times 10^{-5}$	150	0.25

<sup>a</sup>Note that the  $V$  magnitude of AG Car is variable within each range of dates (see Table 1 for values for a specific date).

<sup>b</sup>The photometric variability inside each range of epochs, if due to changes in  $L_*$ , imply variations in the value of  $\log(L_*/L_\odot)$  listed above inside each range of epochs by  $\pm 0.02$  dex.

We support the conclusion of Lamers et al. (2001) that the He abundance on the surface of AG Car is higher than in the nebula<sup>12</sup>. In addition, we found, despite the uncertainties, that the ratio N/O is significantly higher on the stellar surface ( $\text{N/O} = 39^{+28}_{-18}$  by number) than in the nebula ( $\text{N/O} = 6 \pm 2$ , Smith et al. 1997). Therefore, we conclude that the surface of the star has more CNO-processed material than the nebula. This is consistent with the idea that the massive nebula is composed of less chemically-processed outer layers which were ejected from the central star. The pre-existing interstellar bub-

ble likely contains negligible amount of material compared to the total mass of the nebula (Lamers et al. 2001). Whether all the nebular mass was ejected in a single giant eruption  $\sim 10^4$  years ago relies on the knowledge of the mass-loss history of AG Car earlier than and during the LBV phase, which is unknown.

The N/O ratio obtained for AG Car is roughly in line with the predictions of the evolutionary models by Meynet & Maeder (2003). A star with an initial mass of  $85 M_\odot$  reaches a similar He content as AG Car at an age of about  $3 \times 10^6$  years, when the evolutionary models predict  $\text{N/O} \simeq 26$  and  $\text{N/O} \simeq 20$  for the non-rotating and rotating cases, respectively. Detailed comparisons between AG Car and evolutionary tracks, and the implications of our results for the current evolutionary scenario

<sup>12</sup> Lamers et al. (2001) used the He abundance of AG Car derived by Smith et al. (1994), which is very similar to the value obtained in this work.

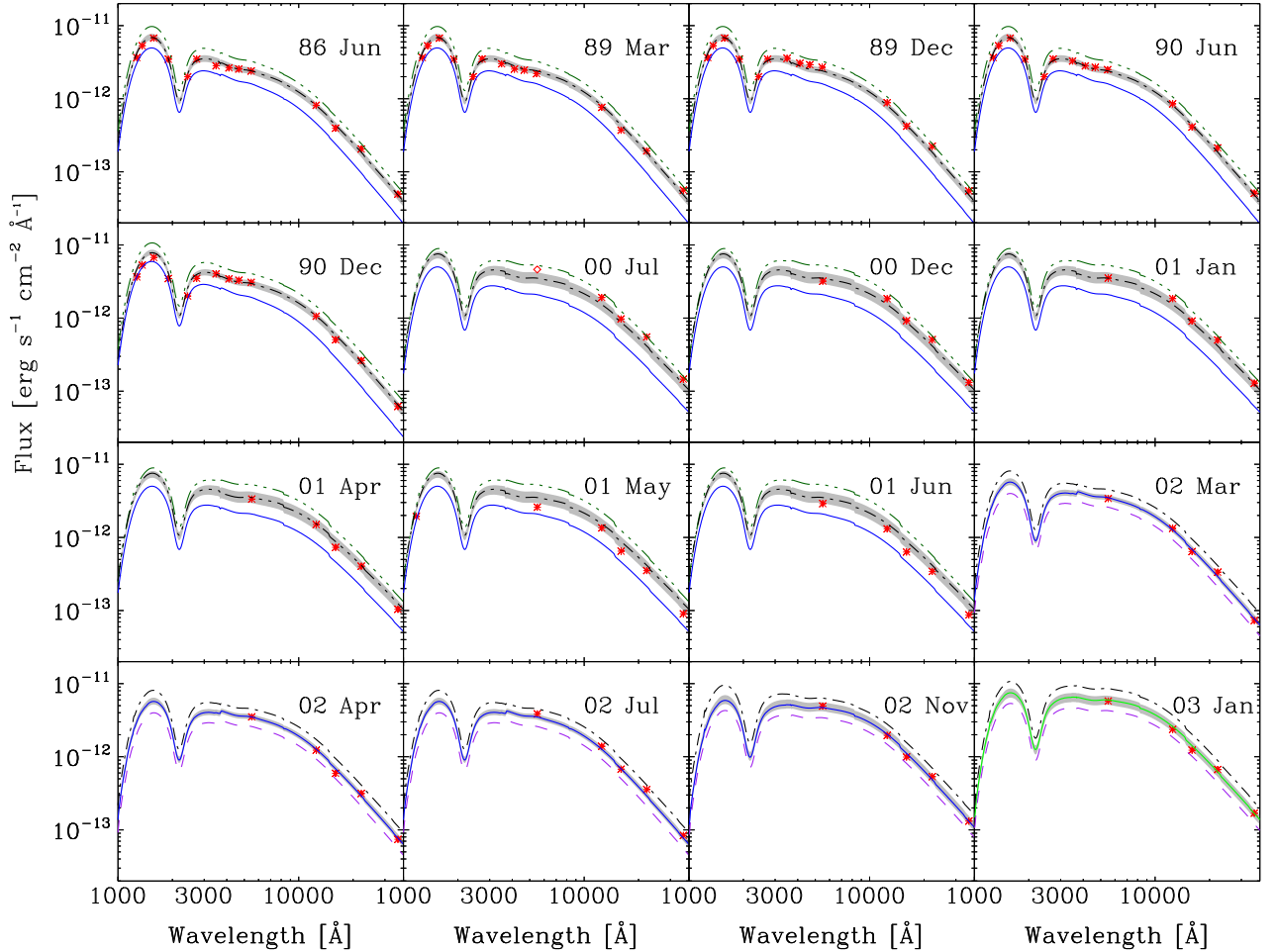


FIG. 11.— Comparison between the observed spectral energy distribution of AG Car obtained from photoelectric data during minimum epochs (red asterisks) and CMFGEN models with different bolometric luminosities. For 2000 July we display the visual magnitude (red open diamond). The panels are ordered chronologically, and in decreasing effective temperature, from left to right, top to bottom. For each panel we show selected models with  $L_{\star} = 2.2 \times 10^6 L_{\odot}$  (dark green dash-triple dotted line),  $L_{\star} = 1.5 \times 10^6 L_{\odot}$  (black dash-dotted line),  $L_{\star} = 1.1 \times 10^6 L_{\odot}$  (light green solid line),  $L_{\star} = 1.0 \times 10^6 L_{\odot}$  (blue solid line), and  $L_{\star} = 0.7 \times 10^6 L_{\odot}$  (purple dashed line). For a given epoch, models with different  $L_{\star}$  had their  $R_{\star}$  and  $\dot{M}$  scaled in order to still fit the observed spectral lines. The gray region corresponds to the uncertainty in the model flux which comes from the luminosity. In all panels, the CMFGEN models were reddened using the Galactic extinction law of Fitzpatrick (1999) with  $R_V = 3.5$  and  $E(B - V) = 0.65$ . For each epoch, there is superb agreement between the best model and the observed data using the same reddening law, although different luminosities are needed. Note the trend towards lower luminosity as the effective temperature (radius) decreases (increases) during 2001–2003. The uncertainty in the observed photometry is smaller than the size of the symbols in the UV, optical, and in the near-IR.

of massive stars will be presented in Paper II.

In the last  $10^4$  years, additional CNO-processed material could have been brought to the surface of AG Car. The star is likely a fast rotator (Groh et al. 2006), suggesting that rotational mixing could efficiently occur due to meridional circulation and shear instability (Maeder & Meynet 2000). In addition, approximately  $0.5 M_{\odot}$  has been removed from the star due to the steady stellar wind since the nebula was ejected, assuming an average mass-loss rate of  $5 \times 10^{-5} M_{\odot} \text{yr}^{-1}$  during the last  $10^4$  years (Paper III).

### 7.2. Comparison with previous works

Fundamental parameters of AG Car during the minimum of 2000–2003 have been presented here for the first time and, therefore, only our results for the minimum

TABLE 6  
COMPARISON BETWEEN SURFACE AND NEBULAR ABUNDANCES OF AG CAR

	He/H (number)	N/O (number)	Reference
Surface	$0.43 \pm 0.08$	$39_{-18}^{+28}$	this work
Nebula	$\sim 0.3^a$	$6 \pm 2$	Smith et al. (1997)

<sup>a</sup>Indirectly obtained by Lamers et al. (2001).

of 1985–1990 can be compared with previous works. We summarize in Table 7 the results obtained by different works.

In general, we derived a higher  $L_{\star}$ , higher  $T_{\star}$ , lower  $T_{\text{eff}}$ , and lower  $\dot{M}$  compared to previous works. These different results are directly or indirectly related to the inclusion of wind clumping, full line blanketing, detailed treatment in non-LTE of the populations and of the ra-

diative field in the co-moving frame, and improved treatment of the subsonic part of the wind in our analysis. The lower mass-loss rates derived by us are a direct consequence of the relatively high degree of clumping found in the wind of AG Car ( $f \simeq 0.1$ ), and the assumption of different  $L$  and  $v_\infty$  by previous authors also affects the value of  $\dot{M}$ . The lower  $\dot{M}$  and higher  $L_\star$  derived by our work implies a reduction in the wind performance number  $\eta = \dot{M}v_\infty c/L$ . During the minimum of 1985–1990 we found a quite modest value of  $\eta \simeq 0.16$ . The increase in  $T_\star$  in our results can be explained by the back-warming of the base of the wind due to the inclusion of line blanketing in our modeling. The significant differences in  $T_{\text{eff}}$  also indicate that obtaining  $T_{\text{eff}}$  from simple empirical relationships, such as using the V-band flux, do not provide a correct answer for hot luminous stars with dense winds, such as AG Car.

The He abundance obtained in this work (He/H =  $0.43 \pm 0.08$ ) is compatible with the value of He/H  $\simeq 0.41$  determined by Smith et al. (1994). All the other abundances have been derived here for the first time, including the detection of CNO-processed material on the surface of AG Car.

The wind terminal velocity derived by us ( $v_\infty \simeq 300 \text{ km s}^{-1}$ ) is higher than the value of  $v_\infty \simeq 250 \text{ km s}^{-1}$  obtained by previous works using the FWHM of optical lines (Leitherer et al. 1994; Smith et al. 1994; Stahl et al. 2001), because we used the saturated absorption profile of resonance lines in the UV to infer  $v_\infty$ , which is a more accurate diagnostic. We found that the optical lines are sensitive to the velocity law, and usually provide a lower limit to  $v_\infty$ . Guo & Li (2007) derived  $\beta = 0.5$  for AG Car during 1990 based on the fitting of the continuum flux, but under the assumption of a series of fixed parameters ( $\dot{M}$ ,  $R_\star$ ,  $T_{\text{eff}}$ ,  $L_\star$ ,  $v_\infty$ ) obtained from Stahl et al. (2001). All these parameters, as well as wind clumping and line blanketing, affect the shape of the continuum, and the assumed values by Guo & Li (2007) are significantly different than the values derived in this paper. Our detailed fits to the line profiles require a much slower velocity law ( $\beta = 3$ ) for the wind of AG Car than that determined by Guo & Li (2007).

### 7.3. On the nature of the changes in the bolometric luminosity during the S-Dor cycle

The evolution of LBVs during the S-Dor cycles is widely *assumed* to occur roughly at constant bolometric luminosity (van Genderen 1979; Stahl et al. 1983; Humphreys et al. 1989; Leitherer et al. 1989, 1994; Smith et al. 1994; Shore et al. 1996; de Koter et al. 1996; Stahl et al. 2001; Vink & de Koter 2002; Walborn et al. 2008). However, the few previous works that investigated changes in the bolometric luminosity of LBVs during the S-Dor cycle (e.g. Humphreys et al. 1989 for AG Car, and Walborn et al. 2008 for R127) employed standard bolometric corrections of OB stars, which we argue are not realistic for LBVs, and photometry restricted to the V-band. For instance, the bolometric corrections obtained in this work for AG Car are more negative by 0.15 to 0.60 mag, depending on the epoch, than those of normal B supergiants (with a similar low  $\log g$ ) obtained using line-blanketed models such as CMFGEN (Crowther et al. 2006) or TLUSTY (Lanz & Hubeny

2007). When compared to the BCs of B supergiants provided by works which employed non-blanketed models, such as Humphreys & McElroy (1984), the BCs derived for AG Car are even more discrepant, being more negative by 0.40 to 0.90 mag, depending on the epoch.

Through a detailed multi-wavelength spectroscopic modeling using CMFGEN, we found in Sect. 6.5 that the bolometric luminosity of AG Car decreases by a factor of 1.5 ( $\sim 0.2$  dex) from minimum towards the maximum phase of the S-Dor cycle Sect. 6.5. Such a finding deserves further discussion, in particular because the variable  $L_\star$  could provide a crucial constraint on the mechanism driving the S-Dor type variability.

A reduction of the bolometric luminosity during the S-Dor cycle was also obtained by Lamers (1995) for the LBV S Doradus, and the result was interpreted in terms of the energy used to expand the outer layers of the star from minimum to maximum. Lamers (1995) found that about  $10^{-3}$  to  $10^{-2} M_\star$  are involved in the expansion of S Doradus, corresponding to  $\sim 0.17 M_\odot$  (assuming  $M_\star \simeq 45 M_\odot$ , Lamers 1995).

We propose that a similar behavior is present in AG Car. In order to obtain an order-of-magnitude estimate of the amount of mass taking part in the expansion of the star, we assume that  $L_\star$  decreased from  $L_\star = 1.5 \times 10^6 L_\odot$  to  $L_\star = 1.0 \times 10^6 L_\odot$  on 2001 June 15 (the last epoch for which we derived  $L_\star = 1.5 \times 10^6 L_\odot$ , see Sect. 6.5), and remained constant until 2003 January 11. The elapsed time  $\Delta t$  between 2001 June 15 and 2003 January 11 is 575 days and, therefore, the missing radiative energy during these epochs is  $\Delta E_{\text{rad}} = \Delta L \cdot \Delta t \simeq 1 \times 10^{47}$  erg. Assuming that the layer is expanding from  $85 R_\odot$  to  $115 R_\odot$ , and following Lamers (1995),

$$\Delta E_{\text{rad}} = \frac{GM_{\text{exp}}M_{\text{eff}}}{R_\odot} \left\{ \frac{1}{85} - \frac{1}{115} \right\}, \quad (2)$$

where  $M_{\text{eff}} = M_\star(1 - \Gamma)$ . Since our CMFGEN models predict that  $\Gamma \simeq 0.8$ , we obtain  $M_{\text{eff}} \simeq 14 M_\odot$  assuming  $M_\star \simeq 70 M_\odot$  (Paper II). Using Eq. 2, we derive that roughly  $8.3 \times 10^{-3} M_\star \sim 0.6 M_\odot$  is involved in the expansion of the star during the S Dor cycle.

This result should be viewed with caution, since an uncertainty of at least a factor of 3 is present due to the various assumptions made above. The amount of  $\sim 0.6 M_\odot$  can be easily increased by a factor of 2 if we include the thermal energy released by the expanding layer (see discussion in Lamers 1995). If we also take into account that we did not analyze in this paper the epochs corresponding to the maximum in the lightcurve of AG Car, which was only reached in 2004–2005 (Paper III), an additional amount of energy would be required, increasing by another factor of  $\sim 2$  the amount of mass involved in the expansion. Therefore, although detailed modeling is obviously needed, it might be possible that  $0.6$  to  $2 M_\odot$  are taking part in the expansion of AG Car during the S-Dor cycle.

Interestingly, such an amount of mass is an order of magnitude lower than the nebular mass found around AG Car ( $\sim 15 - 30 M_\odot$ , Voors et al. 2000) and that of the Homunculus nebula around Eta Car ( $\sim 12 - 20 M_\odot$ , Smith et al. 2003). On the other hand, the amount of mass involved in the S-Dor type variability of AG Car (this work) and S Doradus (Lamers 1995) is comparable

TABLE 7  
 FUNDAMENTAL PARAMETERS OF AG CAR OBTAINED BY DIFFERENT WORKS

1989 March									
Work	$\log L_*/L_\odot$	$T_*$ (K)	$T_{\text{eff}}$ (K)	$Mf^{-0.5}$ ( $10^{-5} M_\odot \text{yr}^{-1}$ )	$v_\infty$ ( $\text{km s}^{-1}$ )	$f$	He/H (number)	$\eta$	$M_V$ (mag)
this	6.17	26,200	22,800	4.7	300	0.1	0.43	0.17	-8.17
SCP94 <sup>a</sup>	6.04	26,000	...	5.6	250	1.0	0.41	0.60	-7.7
1990 December									
Work	$\log L_*/L_\odot$	$T_*$ (K)	$T_{\text{eff}}$ (K)	$Mf^{-0.5}$ ( $10^{-5} M_\odot \text{yr}^{-1}$ )	$v_\infty$ ( $\text{km s}^{-1}$ )	$f$	He/H (number)	$\eta$	$M_V$ (mag)
this	6.17	24,640	21,500	4.7	300	0.1	0.43	0.17	-8.46
LEI94 <sup>b</sup>	6.00	...	21,000	10.0	250	1.0	1.00	1.42	-8.0
STA01 <sup>c</sup>	6.00	...	24,060	3.3	225	1.0	0.41	0.35	-8.0

<sup>a</sup>Smith et al. (1994).

<sup>b</sup>Leitherer et al. (1994).

<sup>c</sup>Stahl et al. (2001).

to the nebular mass found around many low-luminosity LBVs and to that of the Little Homunculus around Eta Car (see Smith & Owocki 2006 and references therein for a compilation of the amount of nebular mass found around LBVs). Such similarity might suggest a link between some of the giant outbursts of LBVs and their S-Dor cycles, and we speculate that the S-Dor cycles could actually be failed Giant Eruptions. Instead of losing several solar masses like Eta Car did in the 1840's, we suggest that during the S-Dor type variability such an amount of mass is never ejected from the star.

## 8. CONCLUSIONS

The detailed spectroscopic analysis of AG Car using the radiative transfer code CMFGEN has provided additional insights on the LBV phenomenon and on the S-Dor type variability. Below we summarize the main conclusions of this paper.

1. Following the determination of a high content of He, N, and Na, and the depletion of H, C, and O, compared to the solar values, we infer that CNO-processed material is present on the surface of AG Car. The actual surface is probably the peeled-off inner layers of the star, which are exposed due to the action of a continuous stellar wind and the ejection of the outer layers due to a giant eruption that occurred  $10^4$  years ago. Since AG Car is likely a fast rotator (Groh et al. 2006), rotational mixing might also have played a role to increase the content of CNO-processed material on the surface. The abundances obtained for Si, Al, Mg, Fe, Ni, Co, Cr, and Mn are consistent with a solar abundance.
2. The minimum phases of the S Dor cycle of AG Car are not equal to each other. The consecutive minimum phases of 1985–1990 and 2000–2003 were different in duration, visual magnitude, stellar temperature, mass-loss rate, and wind terminal velocity. We suggest that these differences arise due to different underlying stellar parameters, which cause different mass-loss rates and wind terminal velocities. In Paper II we will analyze whether the bi-stability mechanism (Pauldrach & Puls 1990; Vink & de Koter 2002) can explain this behavior.
3. The duration of the last two minimum phases of the

S Dor cycle of AG Car and their variability are related to the maximum temperature achieved. The hotter minimum of 1985–1990 was roughly twice as long as the cooler minimum of 2000–2003. On the other hand, AG Car was markedly more variable during 2000–2003 than during 1985–1990.

4. The comparison between the observed flux of AG Car from the ultraviolet to the near-infrared with the model flux yielded a color excess of  $E(B - V) = 0.65 \pm 0.01$ , with  $R_V = 3.5 \pm 0.1$ . The value of  $R_V$  is consistent with the presence of large grains in the circumstellar environment of AG Car (Hyland & Robinson 1991), but it is lower than the value of  $R_V = 3.9$  proposed by Schulte-Ladbeck et al. (1994).
5. The maximum value of the bolometric luminosity obtained during minimum phases was  $L_* = 1.5 \times 10^6 L_\odot$  for an assumed distance of  $d = 6$  kpc. Excluding the uncertainty in the distance, the error in  $L_*$  due to the spectroscopic analysis is around 10%.
6. Contrary to the current paradigm, we found that  $L_*$  decreases by a factor of 1.5 from minimum as the star moves towards visual maximum of the S-Dor cycle. Since further reduction in  $T_{\text{eff}}$  occurs during maximum (Paper III), it might be possible that  $L_*$  decreases even more during the maximum of the lightcurve.
7. Assuming that the decrease in the bolometric luminosity of AG Car is due the energy used to expand the outer layers of the star (Lamers 1995), we found that roughly  $0.6 - 2 M_\odot$  are involved in the expansion. Although that is much lower than the nebular mass found around AG Car and that the mass of the Homunculus around Eta Car, the amount of mass involved in the S-Dor type variability of AG Car is comparable to the nebular mass found around many low-luminosity LBVs and to that of the Little Homunculus around Eta Car. Such similarity might suggest a link between some of the giant outbursts of LBVs and their strong variability during the S-Dor cycles. We speculate that the S-Dor type instability could be a failed Gi-

ant Eruption, with the several solar masses never being released from the star.

We thank an anonymous referee for providing a very detailed list of comments and suggestions which improved the quality of the original manuscript. We are grateful to Otmar Stahl, Nolan Walborn, Edward Fitzpatrick, and Paul Crowther for kindly providing published digital spectra of AG Car. Thanks also to Ted Gull and Krister Nielsen for insightful discussions about the nature of the absorption lines of AG Car and for communicating results in advance of publication. We thank Michelle Fekety for proofreading the paper. JHG and AD thank Brazilian Agencies FAPESP (grant 02/11446-5) and CNPq (grant 200984/2004-7). JHG also thanks the Max-Planck-Gesellschaft (MPG) for partial financial support for this work. DJH gratefully acknowl-

edges partial support for this work from NASA-LTSA grant NAG5-8211. JHG thanks DJH and the University of Pittsburgh for hospitality and partial support for this work. Some of the data presented in this paper were obtained from the Multimission Archive at the Space Telescope Science Institute (MAST). STScI is operated by the Association of Universities for Research in Astronomy, Inc., under NASA contract NAS5-26555. Support for MAST for non-HST data is provided by the NASA Office of Space Science via grant NAG5-7584 and by other grants and contracts. We acknowledge with thanks the variable star observations from the AAVSO International Database contributed by observers worldwide and used in this research. This research made use of the Smithsonian NASA/ADS and SIMBAD (CDS/Strasbourg) databases.

*Facilities:* OPD/LNA, IUE, ESO, FUSE, CTIO.

## REFERENCES

- Bagnulo, S., Jehin, E., Ledoux, C., et al. 2003, *The Messenger*, 114, 10
- Bandiera, R., Focardi, P., Altamore, A., Rossi, C., & Stahl, O. 1989, in *Astrophysics and Space Science Library*, Vol. 157, IAU Colloq. 113: *Physics of Luminous Blue Variables*, ed. K. Davidson, A. F. J. Moffat, & H. J. G. L. M. Lamers, 279
- Blum, R. D., Conti, P. S., & Daminieli, A. 2000, *AJ*, 119, 1860
- Blum, R. D., Daminieli, A., & Conti, P. S. 2001, *AJ*, 121, 3149
- Bouret, J.-C., Lanz, T., & Hillier, D. J. 2005, *A&A*, 438, 301
- Bouret, J.-C., Lanz, T., Hillier, D. J., et al. 2003, *ApJ*, 595, 1182
- Brand, J. & Blitz, L. 1993, *A&A*, 275, 67
- Bresolin, F., Kudritzki, R.-P., Najarro, F., Gieren, W., & Pietrzyński, G. 2002, *ApJ*, 577, L107
- Busche, J. R. & Hillier, D. J. 2005, *AJ*, 129, 454
- Caputo, F. & Viotti, R. 1970, *A&A*, 7, 266
- Carter, B. S. 1990, *MNRAS*, 242, 1
- Catala, C., Kunasz, P. B., & Praderie, F. 1984, *A&A*, 134, 402
- Clark, J. S., Larionov, V. M., & Arkharov, A. 2005, *A&A*, 435, 239
- Conti, P. S. 1984, in *IAU Symp. 105: Observational Tests of the Stellar Evolution Theory*, ed. A. Maeder & A. Renzini, 233
- Crowther, P. A. 1997, in *ASP Conf. Ser. 120: Luminous Blue Variables: Massive Stars in Transition*, ed. A. Nota & H. Lamers, 51
- Crowther, P. A. 2006, in *Astronomical Society of the Pacific Conference Series*, Vol. 348, *Astrophysics in the Far Ultraviolet: Five Years of Discovery with FUSE*, ed. G. Sonneborn, H. W. Moos, & B.-G. Andersson, 107
- Crowther, P. A. 2007, *ARA&A*, 45, 177
- Crowther, P. A., Lennon, D. J., & Walborn, N. R. 2006, *A&A*, 446, 279
- Crowther, P. A., Hillier, D. J., Evans, C. J., et al. 2002, *ApJ*, 579, 774
- Davies, B., Oudmaijer, R. D., & Vink, J. S. 2005, *A&A*, 439, 1107
- Davies, B., Oudmaijer, R. D., & Vink, J. S. 2006, in *ASP Conf. Ser. 355: Stars with the B[e] Phenomenon*, ed. M. Kraus & A. S. Miroshnichenko, 173
- Davies, B., Vink, J., & Oudmaijer, R. 2008, in *ASP Conf. Series*, Vol. 388, *Mass Loss From Stars and The Evolution of Stellar Clusters*, ed. A. de Koter, L. J. Smith, & L. B. F. M. Lamers, 71
- Davies, B., Vink, J. S., & Oudmaijer, R. D. 2007, *A&A*, 469, 1045
- de Freitas Pacheco, J. A., Daminieli Neto, A., Costa, R. D. D., & Viotti, R. 1992, *A&A*, 266, 360
- de Koter, A., Lamers, H. J. G. L. M., & Schmutz, W. 1996, *A&A*, 306, 501
- de Wit, W. J., Testi, L., Palla, F., & Zinnecker, H. 2005, *A&A*, 437, 247
- Drissen, L., Crowther, P. A., Smith, L. J., et al. 2001, *ApJ*, 546, 484
- Feldmeier, A. 1995, *A&A*, 299, 523
- Fich, M., Blitz, L., & Stark, A. A. 1989, *ApJ*, 342, 272
- Figer, D. F., Najarro, F., Morris, M., et al. 1998, *ApJ*, 506, 384
- Figuerêdo, E., Blum, R. D., Daminieli, A., & Conti, P. S. 2002, *AJ*, 124, 2739
- Figuerêdo, E., Blum, R. D., Daminieli, A., Conti, P. S., & Barbosa, C. L. 2008, *AJ*, 136, 221
- Fitzpatrick, E. L. 1999, *PASP*, 111, 63
- Gies, D. R. 1987, *ApJS*, 64, 545
- Gräfener, G. & Hamann, W.-R. 2008, *A&A*, 482, 945
- Grevesse, N., Asplund, M., & Sauval, A. J. 2007, *Space Science Reviews*, 130, 105
- Groh, J. H., Daminieli, A., & Hillier, D. J. 2008, in *Revista Mexicana de Astronomia y Astrofisica Conference Series*, Vol. 33, 132
- Groh, J. H., Daminieli, A., & Jablonski, F. 2007, *A&A*, 465, 993
- Groh, J. H., Hillier, D. J., & Daminieli, A. 2006, *ApJ*, 638, L33
- Gull, T. R., Kober, G. V., & Nielsen, K. E. 2006, *ApJS*, 163, 173
- Gull, T. R., Vieira, G., Bruhweiler, F., et al. 2005, *ApJ*, 620, 442
- Guo, J. H. & Li, Y. 2007, *ApJ*, 659, 1563
- Hamann, W.-R., Gräfener, G., & Liermann, A. 2006, *A&A*, 457, 1015
- Herald, J. E., Hillier, D. J., & Schulte-Ladbeck, R. E. 2001, *ApJ*, 548, 932
- Hillier, D. J. 1987, *ApJS*, 63, 947
- Hillier, D. J. 1989, *ApJ*, 347, 392
- Hillier, D. J. 1990, *A&A*, 231, 116
- Hillier, D. J., Crowther, P. A., Najarro, F., & Fullerton, A. W. 1998, *A&A*, 340, 483
- Hillier, D. J., Davidson, K., Ishibashi, K., & Gull, T. 2001, *ApJ*, 553, 837
- Hillier, D. J., Gull, T., Nielsen, K., et al. 2006, *ApJ*, 642, 1098
- Hillier, D. J., Lanz, T., Heap, S. R., et al. 2003, *ApJ*, 588, 1039
- Hillier, D. J. & Miller, D. L. 1998, *ApJ*, 496, 407
- Hillier, D. J. & Miller, D. L. 1999, *ApJ*, 519, 354
- Hoekzema, N. M., Lamers, H. J. G. L. M., & van Genderen, A. M. 1992, *A&A*, 257, 118
- Hubeny, I., Steff, S., & Harmanec, P. 1985, *Bulletin of the Astronomical Institutes of Czechoslovakia*, 36, 214
- Humphreys, R. M. 1970, *PASP*, 82, 1161
- Humphreys, R. M. & Davidson, K. 1994, *PASP*, 106, 1025
- Humphreys, R. M., Lamers, H. J. G. L. M., Hoekzema, N., & Cassatella, A. 1989, *A&A*, 218, L17
- Humphreys, R. M. & McElroy, D. B. 1984, *ApJ*, 284, 565
- Hyland, A. R. & Robinson, G. 1991, *Proceedings of the Astronomical Society of Australia*, 9, 124
- Johansson, S., Gull, T. R., Hartman, H., & Letokhov, V. S. 2005, *A&A*, 435, 183
- Kauffer, A., Stahl, O., Tubbesing, S., et al. 1999, *The Messenger*, 95, 8
- Lamers, H. J. G. L. M. 1995, in *Astronomical Society of the Pacific Conference Series*, Vol. 83, *IAU Colloq. 155: Astrophysical Applications of Stellar Pulsation*, ed. J. Matthews, 176

- Lamers, H. J. G. L. M., Nota, A., Panagia, N., Smith, L. J., & Langer, N. 2001, *ApJ*, 551, 764
- Lanz, T. & Hubeny, I. 2007, *ApJS*, 169, 83
- Leitherer, C., Allen, R., Altner, B., et al. 1994, *ApJ*, 428, 292
- Leitherer, C., Schmutz, W., Abbott, D. C., Hamann, W.-R., & Wessolowski, U. 1989, *ApJ*, 346, 919
- Maeder, A. & Meynet, G. 2000, *ARA&A*, 38, 143
- Manfroid, J., Sterken, C., Bruch, A., et al. 1991, *A&AS*, 87, 481
- Manfroid, J., Sterken, C., Cunow, B., et al. 1995, *A&AS*, 109, 329
- Marcolino, W. L. F., de Araújo, F. X., Lorenz-Martins, S., & Fernandes, M. B. 2007, *AJ*, 133, 489
- Martins, F., Schaerer, D., & Hillier, D. J. 2005, *A&A*, 436, 1049
- McGregor, P. J., Finlayson, K., Hyland, A. R., et al. 1988a, *ApJ*, 329, 874
- McGregor, P. J., Hyland, A. R., & Hillier, D. J. 1988b, *ApJ*, 324, 1071
- Meynet, G. & Maeder, A. 2000, *A&A*, 361, 101
- Meynet, G. & Maeder, A. 2003, *A&A*, 404, 975
- Mitra, P. M. & Dufour, R. J. 1990, *MNRAS*, 242, 98
- Najarro, F. 2001, in *Astronomical Society of the Pacific Conference Series*, Vol. 233, P Cygni 2000: 400 Years of Progress, ed. M. de Groot & C. Sterken, 133
- Najarro, F., Figer, D. F., Hillier, D. J., Geballe, T. R., & Kudritzki, R. P. 2009, *ApJ*, 691, 1816
- Najarro, F., Hillier, D. J., Kudritzki, R. P., et al. 1994, *A&A*, 285, 573
- Najarro, F., Hillier, D. J., & Stahl, O. 1997, *A&A*, 326, 1117
- Nielsen, K. E., Gull, T. R., & Vieira Kober, G. 2005, *ApJS*, 157, 138
- Nota, A., Leitherer, C., Clampin, M., Greenfield, P., & Golimowski, D. A. 1992, *ApJ*, 398, 621
- Nota, A., Livio, M., Clampin, M., & Schulte-Ladbeck, R. 1995, *ApJ*, 448, 788
- Owocki, S. P., Castor, J. I., & Rybicki, G. B. 1988, *ApJ*, 335, 914
- Pauldrach, A. W. A. & Puls, J. 1990, *A&A*, 237, 409
- Pellerin, A., Fullerton, A. W., Robert, C., et al. 2002, *ApJS*, 143, 159
- Pojmanski, G. 2002, *Acta Astronomica*, 52, 397
- Prantzos, N., Doom, C., de Loore, C., & Arnould, M. 1986, *ApJ*, 304, 695
- Prinja, R. K., Barlow, M. J., & Howarth, I. D. 1990, *ApJ*, 361, 607
- Puls, J., Markova, N., Scuderi, S., et al. 2006, *A&A*, 454, 625
- Schmutz, W., Hamann, W.-R., & Wessolowski, U. 1989, *A&A*, 210, 236
- Schulte-Ladbeck, R. E., Clayton, G. C., Hillier, D. J., Harries, T. J., & Howarth, I. D. 1994, *ApJ*, 429, 846
- Schulte-Ladbeck, R. E., Schmid, H. M., Meade, M. R., et al. 1997, in *ASP Conf. Ser. 120: Luminous Blue Variables: Massive Stars in Transition*, ed. A. Nota & H. Lamers, 113
- Shore, S. N., Altner, B., & Waxin, I. 1996, *AJ*, 112, 2744
- Smith, L. J., Crowther, P. A., & Prinja, R. K. 1994, *A&A*, 281, 833
- Smith, L. J., Stroud, M. P., Esteban, C., & Vilchez, J. M. 1997, *MNRAS*, 290, 265
- Smith, N., Gehrz, R. D., Hinz, P. M., et al. 2003, *AJ*, 125, 1458
- Smith, N. & Owocki, S. P. 2006, *ApJ*, 645, L45
- Spoon, H. W. W., de Koter, A., Sterken, C., Lamers, H. J. G. L. M., & Stahl, O. 1994, *A&AS*, 106, 141
- Stahl, O. 1986, *A&A*, 164, 321
- Stahl, O., Jankovics, I., Kovács, J., et al. 2001, *A&A*, 375, 54
- Stahl, O., Kaufer, A., & Tubbings, S. 1999, in *ASP Conf. Ser. 188: Optical and Infrared Spectroscopy of Circumstellar Matter*, 331
- Stahl, O., Mandel, H., Wolf, B., et al. 1993, *A&AS*, 99, 167
- Stahl, O., Wolf, B., Klare, G., et al. 1983, *A&A*, 127, 49
- Sterken, C. 1983, *The Messenger*, 33, 10
- Sterken, C., Jones, A., Vos, B., et al. 1996, *Informational Bulletin on Variable Stars*, 4401, 1
- Sterken, C., Manfroid, J., Anton, K., et al. 1993, *A&AS*, 102, 79
- Sterken, C., Stahl, O., Wolf, B., Szeifert, T., & Jones, A. 1995, *A&A*, 303, 766
- van Genderen, A. M. 1979, *A&AS*, 38, 381
- van Genderen, A. M. 1982, *A&A*, 112, 61
- van Genderen, A. M. 2001, *A&A*, 366, 508
- van Genderen, A. M., de Groot, M., & Sterken, C. 1997a, *A&AS*, 124, 517
- van Genderen, A. M., Sterken, C., & de Groot, M. 1997b, *A&A*, 318, 81
- van Genderen, A. M., The, P. S., Augusteijn, T., et al. 1988, *A&AS*, 74, 453
- van Genderen, A. M., The, P. S., Heemskerck, M., et al. 1990, *A&AS*, 82, 189
- Vink, J. S. & de Koter, A. 2002, *A&A*, 393, 543
- Viotti, R. 1971, *PASP*, 83, 170
- Viotti, R., Baratta, G. B., Rossi, C., & di Fazio, A. 1991, in *IAU Symposium, Vol. 143, Wolf-Rayet Stars and Interrelations with Other Massive Stars in Galaxies*, ed. K. A. van der Hucht & B. Hidayat, 499
- Viotti, R., Polcaro, F. V., & Rossi, C. 1993, *A&A*, 276, 432
- Voors, R. H. M., Waters, L. B. F. M., de Koter, A., et al. 2000, *A&A*, 356, 501
- Walborn, N. R. & Fitzpatrick, E. L. 2000, *PASP*, 112, 50
- Walborn, N. R., Fullerton, A. W., Crowther, P. A., et al. 2002, *ApJS*, 141, 443
- Walborn, N. R., Stahl, O., Gamen, R. C., et al. 2008, *ApJ*, 683, L33
- Whitelock, P. A., Carter, B. S., Roberts, G., Whittet, D. C. B., & Baines, D. W. T. 1983, *MNRAS*, 205, 577
- Wolf, B. 1989, *A&A*, 217, 87
- Wolf, B. & Stahl, O. 1982, *A&A*, 112, 111